

Integrating 3D basin modelling concept to determine source rock maturation in the F-O Gas Field, Bredasdorp Basin (offshore South Africa)

by

Lerato Priscilla RAMPHAKA



*Mini-thesis presented for the degree of Master of Science (Petroleum Geosciences) in the Faculty of Natural Sciences
at the
University of the Western Cape*

Supervisor: Prof Tapas Chatterjee
Co-supervisor: Dr Wasiu A. Sonibare

December 2015

Declaration

I, _____ hereby confirm that this work submitted for assessment is my own original work and expressed with my own words. Any uses within it of the works of other authors in any form (e.g. ideas, equations, figures, text, tables and programs) are properly acknowledged. A list of references employed is also included.

Signed.....

Date.....

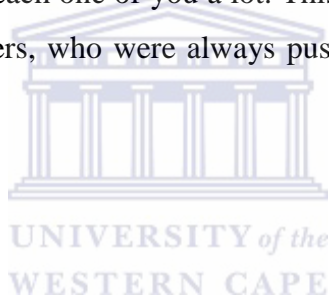


Acknowledgements

I would like to acknowledge support from my supervisors Prof. Tapas Chatterjee and Dr Wasiu Sonibare. I especially wish to thank Dr Wasiu Sonibare for his continuous academic guidance and mentorship as well as encouraging me never to give up throughout the research; this thesis wouldn't be possible without your continuous ideas to help complete it. Thanks Tamlyn for organising the thesis and ideas on how to put it together.

I would like to thank my fellow Petroleum research students, for your continuous support in the two years I have been part of the UWC Earth Science community. A big thank you to all my friends and my brethren from church for praying with and for me, your continuous prayers and the words you ministered really kept me going. My deepest appreciation to my Pastor, there is no way I would have been here without your teachings. I would like to thank my parents and family for their continuous support, I really appreciate and love each one of you a lot. This work is dedicated to my Mother and more especially my two Grandmothers, who were always pushing me to finish this thesis so I can come back home.

Lerato



Executive Summary

The burial history, thermal maturity and petroleum generation history of the F-O Gas Field, Bredasdorp Basin have been studied using 3D basin and petroleum systems modelling approach. The investigated sedimentary basin for this study evolved around mid-late Jurassic to early Cretaceous times when Southern Africa rifted from South America. The F-O field is located 40 km SE of the F-A platform which supplies gas and condensate to the PetroSA 'Gas to Liquid' plant located in Mossel Bay. As data integration is an integral part of the applied modelling concept, 2D seismic profile and well data (i.e. logs and reports from four drilled wells) were integrated into a 3D structural model of the basin.

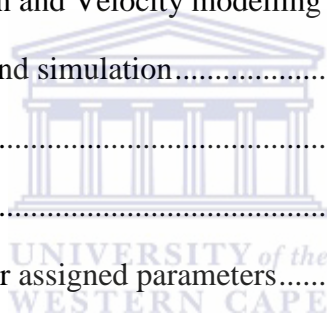
Four source rock intervals (three from the Early Cretaceous stages namely; Hauterivian, Barremian, Aptian and one from the Late Cretaceous Turonian stage) were incorporated into the 3D model for evaluating source rock maturation and petroleum generation potential of the F-O Gas Field. Additionally, measured present-day temperature, vitrinite reflectance, source potential data, basin burial and thermal history and timing of source rock maturation, petroleum generation and expulsion were forwardly simulated using a 3D basin modelling technique. At present-day, Turonian source rock is mainly in early oil (0.55-0.7% VRo) window, while the Aptian and Barremian source rocks are in the main oil (0.7-1.0% VRo) window, and the Hauterivian source rock is mainly in the main oil (0.7-1.0% VRo) to late oil (1.0-1.3% VRo) window. In the entire four source rock intervals the northern domain of the modelled area show low transformation, indicated by low maturity values that are attributable to less overburden thickness. Petroleum generation begins in later part of Early Cretaceous, corresponding to high heat flow and rapid subsidence/ sedimentation rates. The Barremian and Aptian source rocks are the main petroleum generators, and both shows very high expulsion efficiencies. The modelling results however indicate that the younger Aptian source rock could be regarded as the best source rock out of the four modelled source rocks in the F-O field due to its quantity (i.e. highest TOC of 3%), quality (Type II with HI values of 400) and highest remaining potential. At present-day, ~1209 Mtons of hydrocarbons were cumulatively generated and peak generation occurred at ~43 Ma with over 581 Mtons generated. Finally, the results of this study can directly be applied for play to prospect risk analysis of the F-O gas field.

Keywords: Maturity, burial history, hydrocarbon generation, time of generation.

Table of content

Declaration	ii
Acknowledgements	iii
Executive Summary.....	iv
List of Figures.....	vii
List of Tables.....	ix
Chapter One: Introduction.....	1
1.1 Study background.....	1
1.2 Location of Study area	1
1.3 Research Aims and Objectives.....	4
Chapter Two: Regional Setting	5
2.1 Regional Geology.....	5
2.2 Structural and Stratigraphic setting of the Bredasdorp Basin	5
2.2.1 Structural setting.....	5
2.2.2 Stratigraphic development.....	7
Chapter Three: Literature Review	10
3.1 Source Rock Fundamentals.....	10
3.1.1 Total Organic Carbon (TOC) content.....	10
3.1.2 Kerogen type.....	10
3.1.3 Thermal transformations.....	11
3.1.4 Macerals and vitrinite reflectance.....	13
3.1.5 Hydrocarbon Generation	13
3.2 Source rocks in the Bredasdorp Basin.....	15
3.2.1 Syn-rift source rocks (Late Jurassic)	15
3.2.2 Sequence 1A-4A Source rocks (Valanginian).....	16

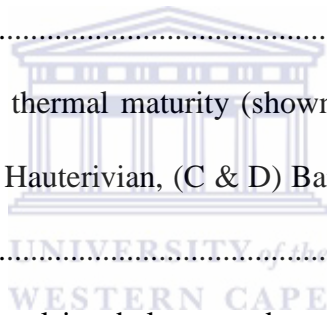
3.2.3 Sequence 5A source rocks (Latest Hauterivian)	16
3.2.4 Sequence 6A-8A Source rocks (Early Barremian).....	16
3.2.5 Sequences 9A-12A source rocks (Late Barremian)	16
3.2.6 Sequence 13A source rocks (Early Aptian).....	17
3.2.7 Sequence 15A source rocks (Early Turonian).....	17
Chapter Four: Methodology	18
4.1 Database	18
4.1.1 Data.....	18
4.1.2 Data Summary	19
4.2 Research Workflow	20
4.2.1 Seismic interpretation and Velocity modelling	20
4.2.2 3D Model building and simulation.....	21
1. Age Assignment	22
2. Paleo-geometries	22
3. Source rocks and their assigned parameters.....	24
Chapter Five: Results and Discussion	26
5.1 Source Rock Maturation.....	26
5.1.1 Thickness Maps	26
5.1.2 Thermal calibration.....	29
5.1.3 Burial and thermal plots	29
5.1.4 Transformation ratio and maturity.....	36
5.2 Petroleum Generation and Expulsion Efficiency	40
Chapter Six: Conclusion and Recommendations	45
References	46



List of Figures

Figure 1. Locality map of the Outeniqua Basin and onshore Mesozoic sedimentary basins in South Africa.	2
Figure 2. Map showing the location of the Bredasdorp basin and its adjacent basins, including the deeper southern Outeniqua Basin. The F-O tract is indicated in the Block 9 of the Bredasdorp Basin in relation with other block in the greater Outeniqua Basin.	3
Figure 3. The location of the F-O field in relation with other producing fields (Sable, Oribi and Oryx) (A) as well as the location of the wells (B) in the F-O field.	4
Figure 4. Distribution of rift basins within the southwest Gondwana before the breakup of Gondwana.	6
Figure 5. Schematic section across the Bredasdorp basin, with the F-A/F-O by the Infanta Arch.	7
Figure 6. Sequence chronostratigraphic chart of the Bredasdorp Basin showing tectonic stages, major unconformities and generalised lithology for the modelled sedimentary units.....	9
Figure 7. Diagram illustrating the principle conditions and procedures for kerogen formation from biological materials and the kerogen change into petroleum products with increase maturation	12
Figure 8. Classification of kerogens into three broad categories, expresses using the van Krevelen diagram. Elemental composition of organic matter in freshly deposited sediments plotted towards the upper right end of the field (diagenesis stage). With increasing burial, kerogen transformation proceeds during the catagenesis and metagenesis stages.....	15
Figure 9. The spatial relationship of the wells and seismic sections within the outlined study area. .	20
Figure 10. W-E well correlation panel showing different zones based on the combination of gamma ray log and well tops.	21
Figure 11. Seismic composite line showing all the wells and the position of the source rocks in the F-O Gas field.....	23
Figure 12. Integrated workflow developed for the study.....	25

Figure 13. Thickness maps of the major unconformities (A) 1At1; (B) 13At1; (C) 15At1; (D) 17At1. (E) North-South cross-sectional profile through the consistent 3D structural model of the F-O Gas Field indicating the modelled 17 layers with their according vertical and lateral lithofacies distribution and areal distribution of potential source rocks.....	28
Figure 14. Basal heat flow trend over time.	29
Figure 15. Burial history with temperature overlay and cross plot of measured and modelled temperature and vitrinite reflectance at wells: F-O1 (A), F-O2 (B), F-R1 (C) and F-S1 (D). Solid line = modelled; Plus sign = measured. Note F-S1 has no measured VR.	33
Figure 16. Burial history with temperature overlay and cross plot of modelled temperature and vitrinite reflectance at well Pseudo North. Solid line = modelled. Note no measured temperature and vitrinite reflectance.	34
Figure 17. Transformation ratio and thermal maturity (shown as vitrinite reflectance) maps of the four source rocks presently. (A & B) Hauterivian, (C & D) Barremian, (E & F) Aptian and (G & H) Turonian.....	40
Figure 18. Results of generation, expulsion balance and remaining potential over time in all the source rocks.	42
Figure 19. Cross plot showing the amount of hydrocarbons accumulated in each source rock. (A) Hauterivian, (B) Barremian, (C) Aptian and (D) Turonian.	44



List of Tables

Table 1. Data that was used to conduct the research project.

Table 2. General well information.

Table 3. List of seismic sections used in the study.

Table 4. Input parameters for the modelled source rocks intervals in the 3D model.

Table 5. Table showing the amount of hydrocarbons generated and expelled over time.



Chapter One: Introduction

1.1 Study background

Source rocks are critical component for a working petroleum system in sedimentary basins (McCarthy et al., 2011). A source rock is an organic-rich sedimentary rock that is capable of producing or has produced versatile amounts of hydrocarbons to form commercial oil and gas accumulations (McCarthy et al., 2011). The source rock is matured when heated sufficiently, enabling the generation of hydrocarbons. Thus, evaluating source rock maturation becomes an important component of exploration assessment for commercial accumulations of oil and gas before any drilling can be done.

In the Bredasdorp Basin (Figure 2), the early Aptian source rock has been well described (e.g. Davies, 1997; Van der Spuy, 2003; Sonibare et al., 2015; Sonibare et al., *subm.*). This early Aptian source rock thickness can be over 200 m thick occurring over a large areal extent and consisting of organic material that is largely Type II with a Type I component in places (Van der Spuy, 2003). These source rocks are matured such that they have been reported to have provided oil to the producing oilfields such as Oribi and its satellite fields (PASA, 2013). Gas-prone source rocks occur in the north flank wells where F-A gas field is producing, and are likely to be available in the centre of the basin though not traversed (Burden, 1992). In the north-eastern portion of the Bredasdorp, early Aptian source rocks have been encountered in the four wells that were drilled. However, the evaluation of source rock maturation as well as source rock contribution to commercial accumulations in the F-O gas fields is still poorly understood.

1.2 Location of Study area

The Bredasdorp Basin is one of the sub-basins within the Outeniqua Basin (Figure. 1). Geographically, the Outeniqua Basin is the southern offshore basin, which shows a history of strong strike-slip movement during the late Jurassic to early Cretaceous breakup and separation of Gondwanaland (Davies, 1997). The Bredasdorp Basin is currently the most explored and well-studied basin where the most hydrocarbon accumulations were discovered on the South African southern coast.

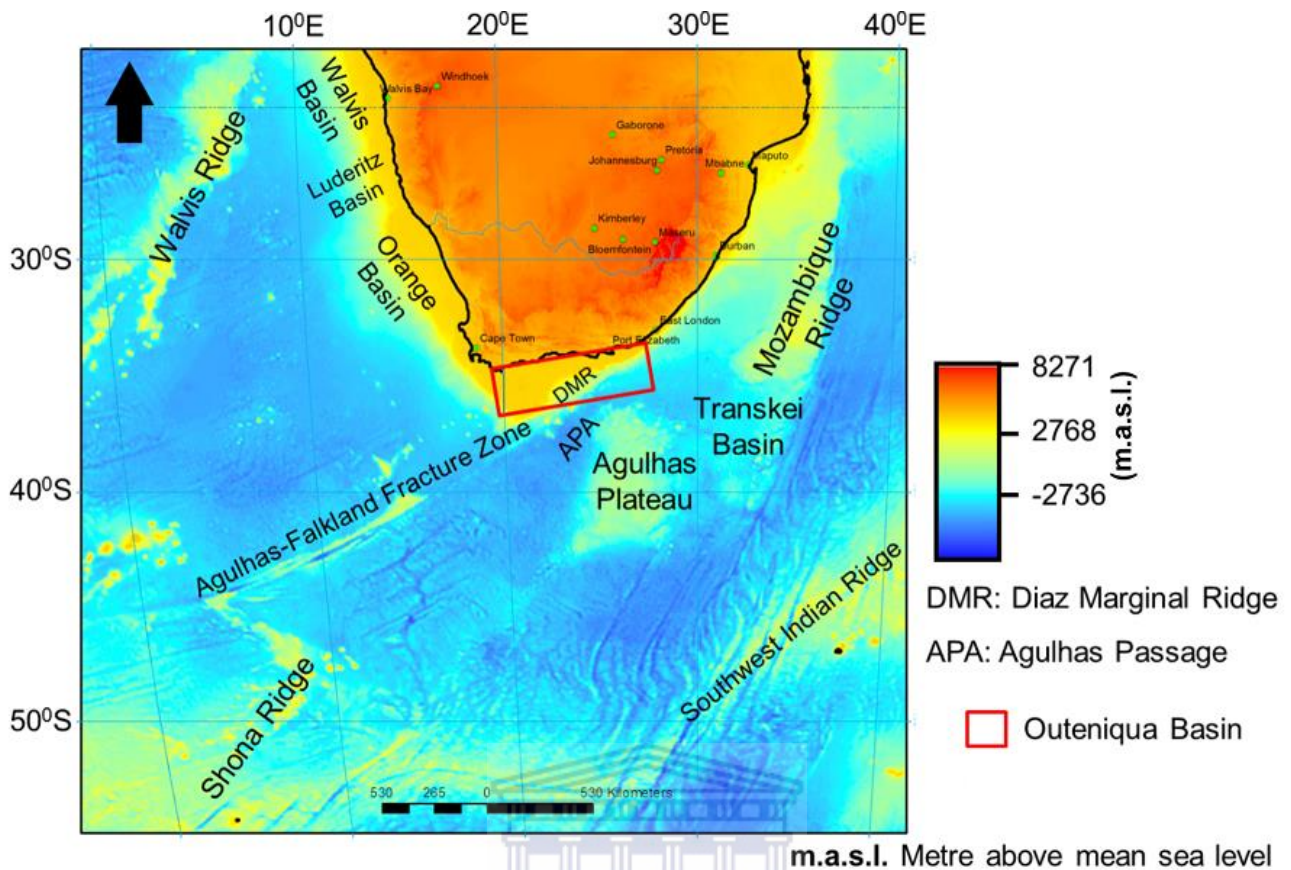


Figure 1. Locality map of the Outeniqua Basin and onshore Mesozoic sedimentary basins in South Africa (adapted from Sonibare et al., 2015).

The Bredasdorp Basin covers an area of approximately 18 000 km², and is filled with continental and marine sediments belonging to Jurassic and Cretaceous age (Davies, 1997). It is bounded on the north-eastern side by the Infanta Arch separating the Bredasdorp Basin from the Pletmos Basin and on the western and south-western side by the Columbine-Agulhas Arch (Megner-Allogo, 2006).

Block 9 of the Bredasdorp Basin is the offshore exploration license area which covers major part of the Bredasdorp Basin. This block is located about 120 km south-west of the Mossel Bay on the Agulhas Bank. The water depth ranges between 100 m and 120 m. The F-O tract, which is located in the eastern part of Block 9 on the north-eastern flank of the Bredasdorp Basin (Figure. 2), constitutes the study locality in this present work. The F-O field is situated 110 km from the nearest landfall and 40 km SE of the F-A platform, which supplies gas and condensate to the PetroSA GTL (Gas to Liquid) plant located in Mossel Bay (Mudaly et al., 2009) (Figure. 3A).

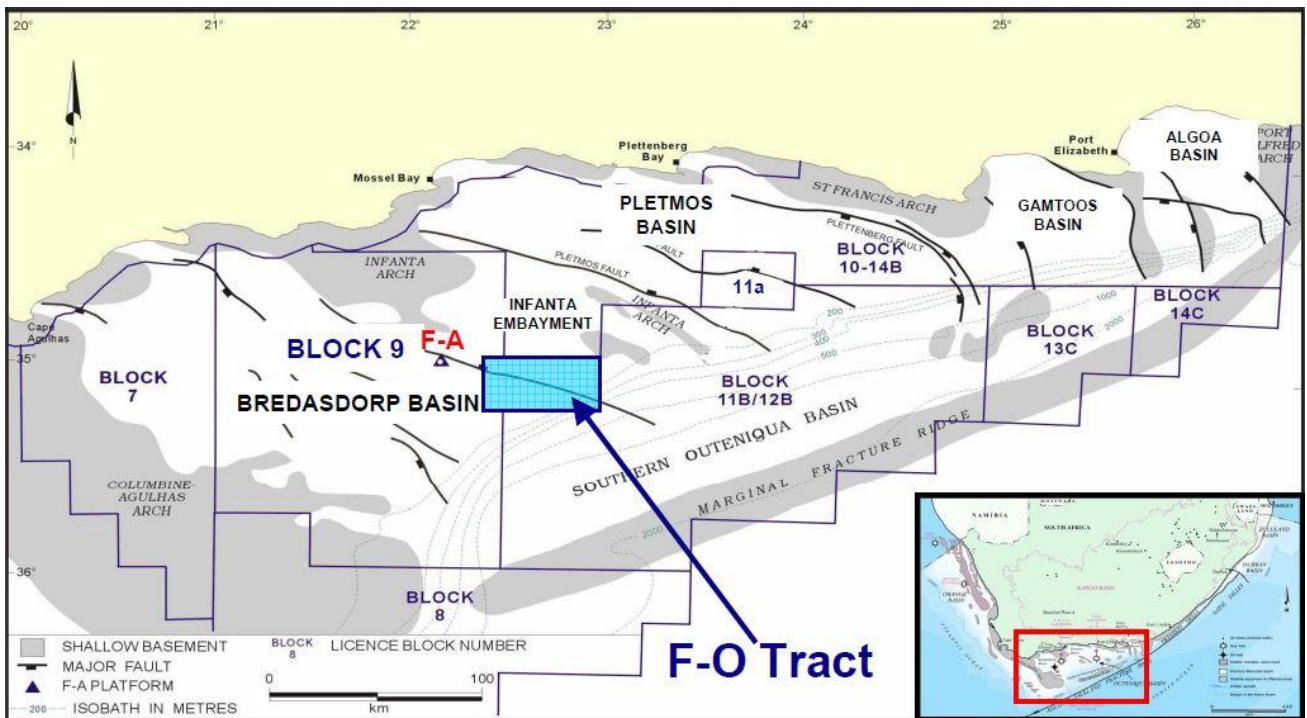


Figure 2. Map showing the location of the Bredasdorp basin and its adjacent basins, including the deeper southern Oudeniqua Basin. The F-O tract is indicated in the Block 9 of the Bredasdorp Basin in relation with other block in the greater Oudeniqua Basin (After Subseaworldnewscom, 2015).

There are four wells that were drilled in the F-O field (Figure. 3B); two of these wells are classified as gas well with potentially commercial production rates. This field is characterised by heterogeneous reservoir with low porosity (2-18%) and permeability (<0.1 to 10 mD). The F-O gas field has some good permeability streaks that reach values of 250 mD. The field is on a well-defined structural high at the level of the regional drift onset unconformity, 1At1 (Mudaly et al., 2009).

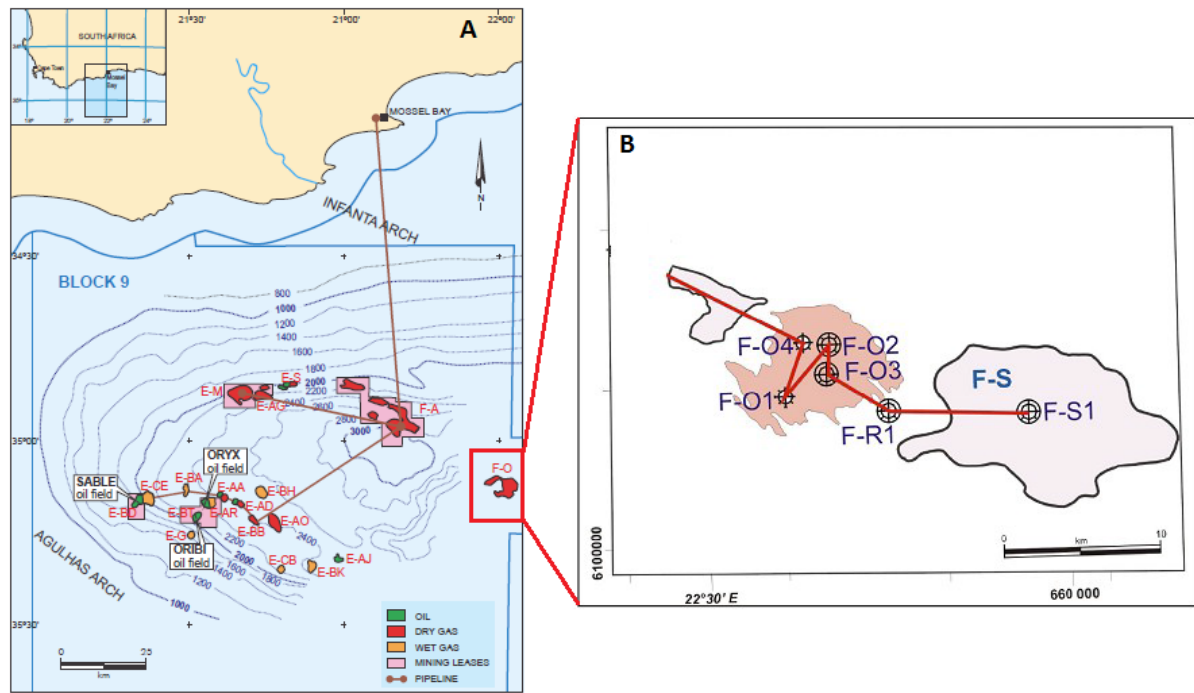


Figure 3. The location of the F-O field in relation with other producing fields (Sable, Oribi and Oryx) (A) as well as the location of the wells (B) in the F-O field (Modified after Broad, 2004 and PASA, 2013).

1.3 Research Aims and Objectives

The primary aim of this project is to evaluate the source rock potential within the F-O gas field in the north-eastern Bredasdorp Basin through the application of 3D basin modelling concept.

In order to accomplish the abovementioned aims, this study implemented the following objectives:

- Identification and interpretation of source rock intervals from 3D seismic survey and well data.
- Incorporation of 3D seismic and well data such as temperature, pressure, lithology, vitrinite reflectance, porosity and permeability from unpublished reports and published literature to construct 3D basin model of the source rock.
- Integration of burial and thermal history plots to predict source rock maturation and hydrocarbon generation as well as to infer tectonic history of the basin.
- Construction of a working model for 3D maturation of the source rock.
- Determination of the amount of hydrocarbon generated over time.

Schlumberger's geological modelling software i.e. Petrel (i.e. seismic to simulation software) and Petromod (petroleum system modelling software) were employed to fully actualise the research aims and objectives of this thesis.

Chapter Two: Regional Setting

2.1 Regional Geology

Gondwana breakup occurred initially in the Early Jurassic with the separation of the West Gondwana consisting of South America and Africa landmasses from the East Gondwana (which consisted of Antarctica, Australia, India and New Zealand (Figure. 4). The separation of the southern Africa and South America occurred in the Mesozoic era resulting in the formation of the continental margin off the south coast of South Africa, thus resulting in the full opening of the greater South Atlantic Margin (Sonibare et al., 2015). This is evidenced by the dextral (right lateral) shear movements along the Agulhas-Falkland Fracture Zone (AFFZ) (McMillan et al., 1997). The aforementioned is thus an important component of the numerous lithospheric stretching and break-up events that characterise the separation of the Gondwanaland supercontinent into the East (Antarctica-Australia-India) and the West (South America-Africa) in the early Mesozoic (Sonibare et al., 2015).

The documented rift phases and tectonic realignments following a series of lithospheric stretching and subsequent thermal relaxation resulted in the formation of five easterly trending en echelon subbasins (Bredasdorp, Infanta Embayment, Pletmos, Gamtoos and Algoa) known collectively as the Outeniqua Basin. These subbasins comprise complex half-graben structures overlain by variable thicknesses of drift sediments (PASA, 2013). The deepwater extensions of these basins (excluding the Algoa Basin) merge into the Southern Outeniqua Basin. The AFFZ separated the great Falkland Plateau from the Outeniqua Basin (Megner-Allogo, 2006) (Figure. 4).

2.2 Structural and Stratigraphic setting of the Bredasdorp Basin

2.2.1 Structural setting

The most prominent structural features of the Bredasdorp Basin are normal faults. The faults show a WNW-ESE trend which have been inherited from the Swartberg Branch of the CFB (Davies, 1997, Johnston, 2000). The normal faults were found to be bounding half-grabens and structural highs throughout the basin (Megner-Allogo, 2006; Sonibare et al., 2015). Majority of the faults are restricted to the rift sequence, though some do extend into the post-rift succession (Davies, 1997; Sonibare et al., 2015). Another set of faults showing a NNW-SSE trend was ascribed to subsequent

shear movement along the Agulhas-Falkland Fracture Zone to the south of the basin (Johnston, 2000; Sonibare et al., 2015).



Figure 4. Distribution of rift basins within the southwest Gondwana before the breakup of Gondwana (after PASA, 2013).

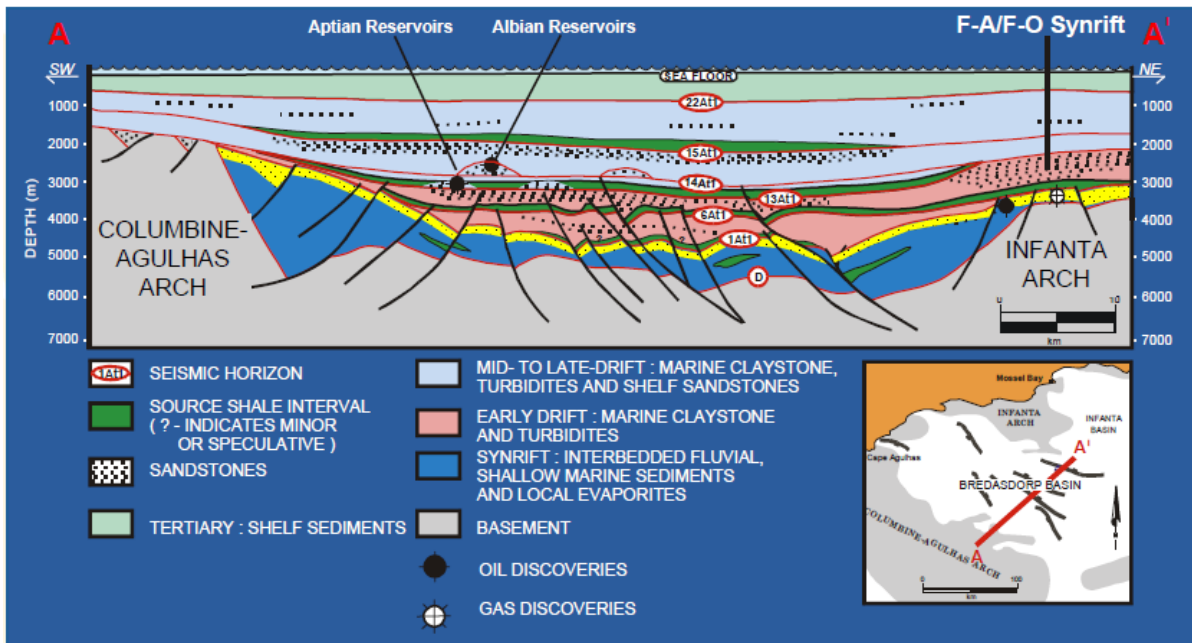


Figure 5. Schematic section across the Bredasdorp basin, with the F-A/F-O by the Infanta Arch (after Mudaly et al., 2009).

2.2.2 Stratigraphic development

The stratigraphic development of the Bredasdorp Basin comprises of four major tectonic phases (see Figure. 6):

1. Mid-Jurassic to Valangian (Basement to 1At1)

Synrift I stage: Extension-driven subsidence initiated by rifting with extensional reactivation of the Cape Fold Belt in Oxfordian and Kimmeridgian times led to the formation of block-faulted synrift basin fill (PASA, 2009; Sonibare et al., 2015). Both sides of the graben have been isostatically inspired bringing about erosional truncation of synrift sediments. Extreme bordering uplift and denudation of the northern side disengaged the Synrift I sedimentary successions in places (PASA, 2009).

2. Late Valangian to Hauterivian (1At1 to 6At1)

Synrift II stage: This stage is characterised by rapid subsidence and far reaching flooding. The synrift II is also regarded as renewed phases of rift tectonics following Valanginian transform processes along the AFFZ (McMillan et al., 1997; Sonibare et al., 2015). Continuous elevation brings about auxiliary of structural highs. Sedimentation commenced within deep water environment

comprises of claystones and siltstones within rift depocenters (Arniston half graben and southern sub basins; PASA, 2009).

3. Hauterivian to Aptian (6At1 to 13Amfs)

Transitional stage: This documents progradational development of shelf in the northern part of the Bredasdorp Basin over the Arniston half-graben, joined with a ceaseless development of the southern sub-basin (PASA, 2009). A major regression phase followed in the early Aptian stage and resulting in significant erosional unconformity in the Bredasdorp Basin (regional 13At1 unconformity). Deposition of deep water marine sediments resulted in the formation of submarine canyons and channels. These canyons and channels provided the path for turbidity flow that fed the lowermost part of the basin, predominantly the Barremian to early Aptian succession between 5At1 and 13At1 in the central part of the basin (Burden, 1992; Davies, 1997; Figure. 6). The development of a stable depositional environment characterised by low sedimentation rates and sediment starvation favoured the deposition of organic-rich mud (Davies, 1997). These muds were deposited as intercalations particularly between 1At1 and 13At1 stratigraphic markers (Figure. 6) and found to be the thickest and best quality source rocks in the basin (Burden, 1992).

4. Late Albian to Cenozoic (13Amfs to Present-day Seafloor)

Post-rift (early to late drift) stage: The post rift stage is primarily characterised by regional subsidence occasioned by thermal subsidence (PASA, 2009). During the late Cenomanian sediment starvation resulted again after the 15At1 unconformity. This was followed by the deposition of organic muds, but was immature to generate hydrocarbons (McMillan et al., 1997). Late Cretaceous and Tertiary sediments are of shelf origin and are generally interbedded calcareous sandstones and marine claystones. By the end of Cretaceous, open shelf conditions prevailed over the entire Bredasdorp Basin. The equivalent deepwater sediments are present to the southeast in the Southern Outeniqua Basin. There is some evidence for uplift, inversion, and folding having occurred during this post-rift stage of the Bredasdorp Basin. During early Tertiary, numerous lamprophyric intrusions were emplaced especially in the western and eastern areas of the basin. During this period about 500 to 1000 m of uplift occurred predominantly along the Agulhas arch (Davies, 1997; PASA, 2009; Sonibare et al., 2015) in the southwestern rim of the basin.

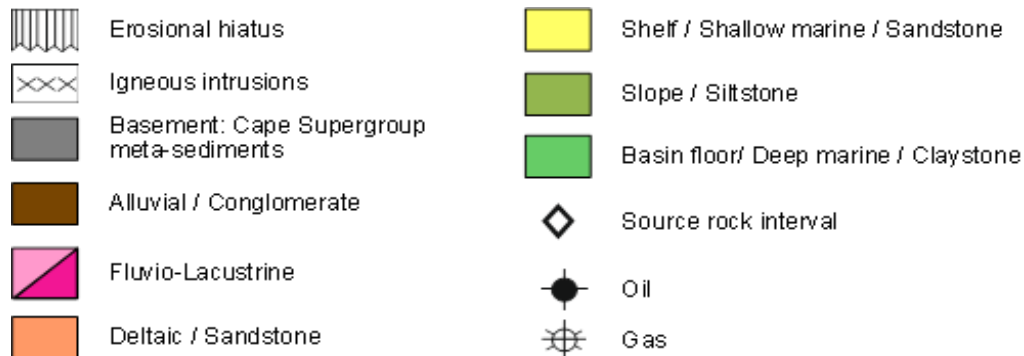
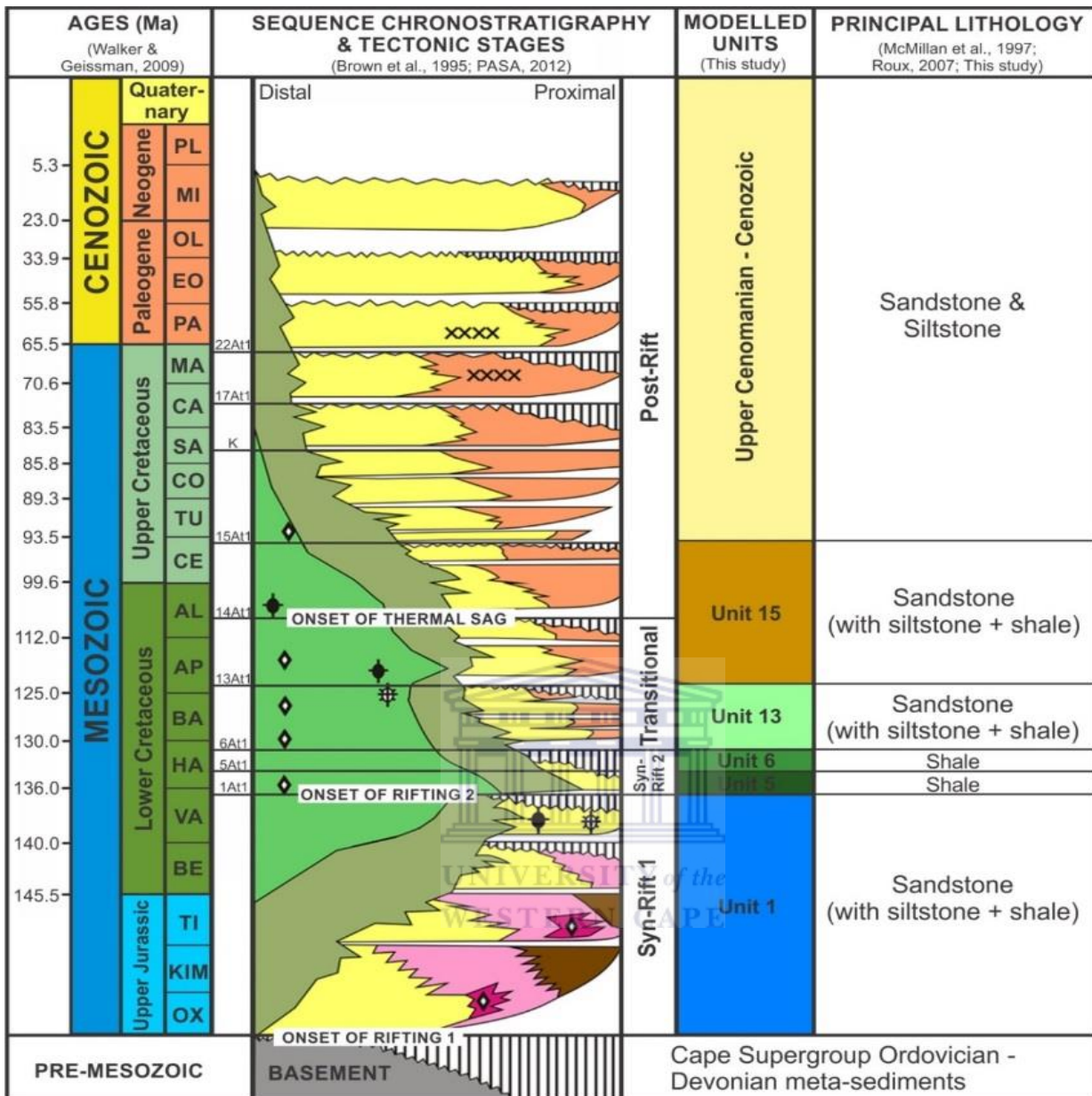


Figure 6. Sequence chronostratigraphic chart of the Bredasdorp Basin showing tectonic stages, major unconformities and generalised lithology for the modelled sedimentary units (adapted from Sonibare et al., 2015).

Chapter Three: Literature Review

3.1 Source Rock Fundamentals

Every oil or gas play originates from source rocks. The viability of each play conventional or unconventional depends on its source rocks. Without this source of hydrocarbon, all other components and processes of the petroleum system that are needed to exploit a play become irrelevant (McCarthy et al., 2011). Source rocks can be broadly defined as any fine-grained, organic-rich siliciclastic (mudstones, claystones, shales) or dark coloured carbonate (limestones, marlstones) rocks that are capable of generating petroleum, given sufficient exposure to heat and pressure (McCarthy et al., 2011).

3.1.1 Total Organic Carbon (TOC) content

Source rocks can be described in terms of their total organic carbon (TOC) content. However, not the entire TOC is available to hydrocarbon generation because the conversion of organic matter to hydrocarbons also depends upon the hydrogen balance, i.e. the convertibility of the organic matter (Schmidt, 2004). The TOC content provides an order of magnitude approximation of the quantity of petroleum formed (Schmidt, 2004). The measured TOC is present as a soluble bitumen and insoluble kerogen. Reactive kerogen is composed of a labile (oil prone) and a refractory (gas prone) fraction (Clayton, 1991a). A minimum TOC content for potential source rocks to generate enough petroleum for expulsion to occur is difficult to estimate because several factors besides the quantity are decisive (Schmidt, 2004). A threshold exists since a critical hydrocarbon concentration in the source rock has to be reached before expulsion from the rock is possible (Dow, 1977a). Prior to expulsion, the specific hydrocarbon adsorption capacity of a source rock has to be satisfied. Moreover, sufficient hydrocarbons for the movement of a pressure-driven hydrocarbon phase have to be available. Estimated minimum TOC values are 0.3% for carbonates and 0.5% for shales (Schmidt, 2004). These minimum values apply only to immature source rock samples because in rocks with an advanced maturity the initial TOC content may have been almost three times as high, depending on the type of kerogen (Daly, 1987).

3.1.2 Kerogen type

Sediment slowly cooks as pressure and temperature increase with burial depth. Given sufficient heat, pressure and time, the sediment lithifies and the organic matter contained within transforms into

kerogen. Dow (1977a) defines kerogen as the portion of organic matter in sedimentary rocks that is insoluble in organic solvents. Kerogen type varies depending on the original biological matter composition as well as the provenance (Schmidt, 2004). Kerogen can be classified into four types, based on provenance, as well as on hydrogen, carbon and oxygen content, with each having a distinct kind of hydrocarbons it will produce (McCarthy et al., 2011).

Type I kerogen is predominately lacustrine environments with some cases of marine depositional setting (Dow, 1977a). This is derived from algae and planktons and it is oil prone being very rich in hydrogen and low in oxygen (McCarthy et al., 2011). Type II kerogen is mainly marine and it is found in reducing environment (Dow, 1977a). It is derived primarily from planktons reworked by bacteria. They are also high in hydrogen and low in carbon; and can generate oil and gas (McCarthy et al., 2011). Type III kerogen is derived from terrestrial organic matter which predominates on the continental shelves (Dow, 1977a). This kerogen type has low hydrogen and higher oxygen content, and thus produces dry gas. Type IV kerogen is derived from residual organic matter that is oxidised (Olugbemiro, 1997 in Schmidt, 2004). It has high carbon content and poor in hydrogen, with almost no potential for generating oil or gas (McCarthy et al., 2011).

3.1.3 Thermal transformations

Deposited organic matter passes through five stages to be fossilised namely: microbial degradation, condensation, organic diagenesis, thermal alteration and organic metamorphism (Hunt, 1974 in Schmidt, 2004). Stages one to three occurs during diagenesis, whereas thermal alteration occurs during catagenesis, which is the main phase of hydrocarbon generation, while metagenesis and metamorphism occurs last. Organic metamorphism parallels the sediment metamorphism (Schmidt, 2004). Thus thermal maturation process can be divided into three stages.

1. Diagenesis: Kerogen formation

The formation of kerogen in sediments results from alteration of organic matter as it is deposited and buried and consequently exposed to higher temperature (Schmidt, 2004). Organic rich sediments which consists of a mixture of microorganism, minerals, dead organic material and large amount of water is altered by oxidation and other chemical processes typically at temperatures below approximately 50 degrees Celsius (McCarthy et al., 2011; Schmidt, 2004). Kerogen consists of three components the inert, refractory and the labile portions (Figure. 7).

2. Catagenesis: Petroleum generation

Sediments are buried several kilometres and temperature increases (50 to 150 °C) and pressures (30 to 150 MPa) the source rock matures (Schmidt, 2004). Compaction, water expulsion and porosity and permeability continue decreasing; thermal alteration of organic matter which involves cracking of larger molecules to form small compounds results (Hunt, 1974 in Schmidt, 2004), producing oil and gas. Type I and Type II kerogen within the oil window produce both oil and gas, while Type III which contains refractory chemical nature generates mainly gas (McCarthy et al., 2011; Figure. 7). As temperature, pressure and burial depth increases, the source rock then enters the upper part of the gas window, where secondary cracking of the oil molecules produces wet gas containing methane, propane, ethane and other heavier hydrocarbons (McCarthy et al., 2011).

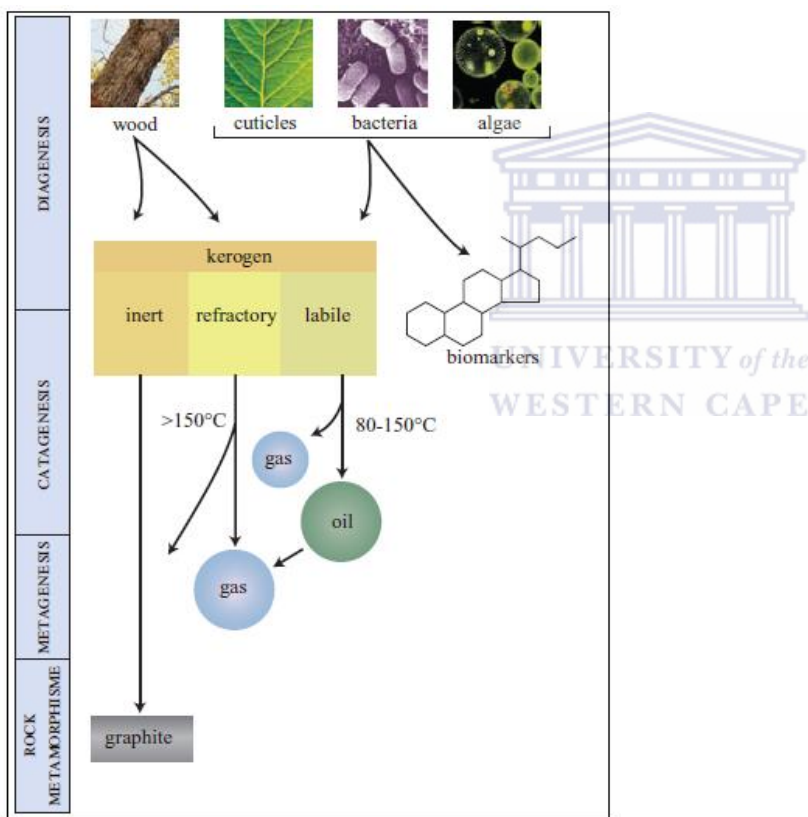


Figure 7. Diagram illustrating the principle conditions and procedures for kerogen formation from biological materials and the kerogen change into petroleum products with increase maturation (Adapted after Leythaeuser, n.d.)

3. Metagenesis and metamorphism: Late gas generation

This is the final stage in which additional heat and chemical changes transform the kerogen into methane and a carbon residue (inert kerogen). With additional heat, the source rock enters the gas

window, producing late dry gas (methane) with nonhydrocarbon gases such as carbon dioxide, nitrogen and hydrogen sulphide (McCarthy et al., 2011). The temperatures for this change, ranges from 150 to 200 °C. Within the carbon residue, crystalline ordering starts developing; thus the transformation of carbon to mineral graphite (Schmidt, 2004) (Figure. 7).

3.1.4 Macerals and vitrinite reflectance

Macerals are components of coals and kerogens which can be comparable to minerals which form rocks (Taylor et al., 1998 in Schmidt, 2004). These are divided according to their reflectivity into three groups: vitrinite, liptinite and inertinite (Schmidt, 2004; Leythaeuser, n.d.). In the present work more emphasis was given to study of the vitrinite. Vitrinite group is principally derived from higher land plants and is essentially made of humified remains of lignin and cellulose of cell walls (Dow, 1977a). The vitrinite macerals are referred as to as humic or structured organic matter (Schmidt, 2004). Vitrinite reflectance data belong to the most important calibration parameter for the maturation history of organic matter and is considered the main parameter for determining the maturity of the sediment rocks (Olugbemi and Ligouis, 1999 in Schmidt, 2004). Vitrinite reflectance evolution is much more sensitive to small temperature changes than most inorganic mineral transformations, irreversible, and not affected by intracratonal solutions or availability of ions (Schmidt, 2004). The vitrinite maceral is mainly used for rank determinations, because its optical properties alter more uniformly during catagenesis than does those of the other maceral groups (Schmidt, 2004). In general, the reflectivity increases with decreasing hydrogen and/or oxygen content (Hunt, 1991 in Schmidt, 2004).

In this study, the EASY% Ro method from Sweeny and Burnham, 1990, was used and adjusted to the study. EASY% Ro is applicable to vitrinite reflectance from Ro 0.30 to 4.5 % = 5.3 % Rmax. Many experimental studies show that type II kerogen source rocks oil window extends over a maturity interval of about 0.5 to 1.3 % vitrinite reflectance (McCarthy et al., 2011). The maturity interval above 1.3 to 2.0 % vitrinite reflectance, hydrocarbons with lower molecular weight such as condensates and wet gases generate (Schmidt, 2004; Leythaeuser, n.d.). Maturity levels that are in excess of 2.0 % vitrinite reflectance only dry gas is generated (Leythaeuser, n.d.). The gradual change from oil to condensate to gas generation occurs is due to the exhaustion of the supply of hydrogen.

3.1.5 Hydrocarbon Generation

Oil and gas are generated by the thermal degradation of kerogen in the source beds. With increasing burial, the temperature in these rocks rises and, above a certain threshold temperature, the chemically

labile portion of the kerogen begins to transform into petroleum compounds (Figure. 7) (Leythaeuser, n.d.). The breaking of carbon-carbon bonds (cracking) is the main reaction mechanism which requires that the input of thermal energy exceed certain minimum levels (activation energy) (Leythaeuser, n.d.). At higher temperature levels, petroleum compounds are generated by the cracking of carbon-carbon bonds within the kerogen structure in such a way that long aliphatic side chains and saturated ring structures are removed from it (Leythaeuser, n.d.). The elemental composition of the kerogen is changed as a result of these reactions especially in a decrease of its hydrogen content. These changes are expressed in the van Krevelen diagram for each kerogen type as trend lines, the so-called evolutionary pathways (Figure. 8).

The generation of oil and gas in source rocks is a natural consequence of the increase of subsurface temperature during geologic time. The process of kerogen transformation with increasing temperatures is called maturation, which is subdivided into the catagenesis and metagenesis stages (Figures 7 & 8, Tissot and Welte, 1984). Organic matter is labelled immature prior to the commencement of hydrocarbon generation, mature if hydrocarbon generation is in progress, or over mature when generation has ended. The main driving force in maturation and hydrocarbon generation is heat. The heating rates as well as the exposure time to maximum temperatures reached are important for maturation determination (Leythaeuser, n.d.). The temperature interval where the oil generation is in progress is referred to as the oil window; this extends from about 50 to 150 °C. It is very essential to determine the precise stage the hydrocarbon generation progressed in a source rock, especially for hydrocarbon exploration. Maturity parameters such as vitrinite reflectance and biomarkers; which record temperature/time integral which the source rocks experienced are used (Leythaeuser, n.d.). Many experimental studies show that type II kerogen source rocks oil window extends over a maturity interval of about 0.5 to 1.3 % vitrinite reflectance (McCarthy et al., 2011). The maturity interval above 1.3 to 2.0 % vitrinite reflectance, hydrocarbons with lower molecular weight such as condensates and wet gases generate (Schmidt, 2004; Leythaeuser, n.d.). Maturity levels that are in excess of 2.0 % vitrinite reflectance only dry gas is generated (Leythaeuser, n.d.). The gradual change from oil to condensate to gas generation occurs is due to the exhaustion of the supply of hydrogen.

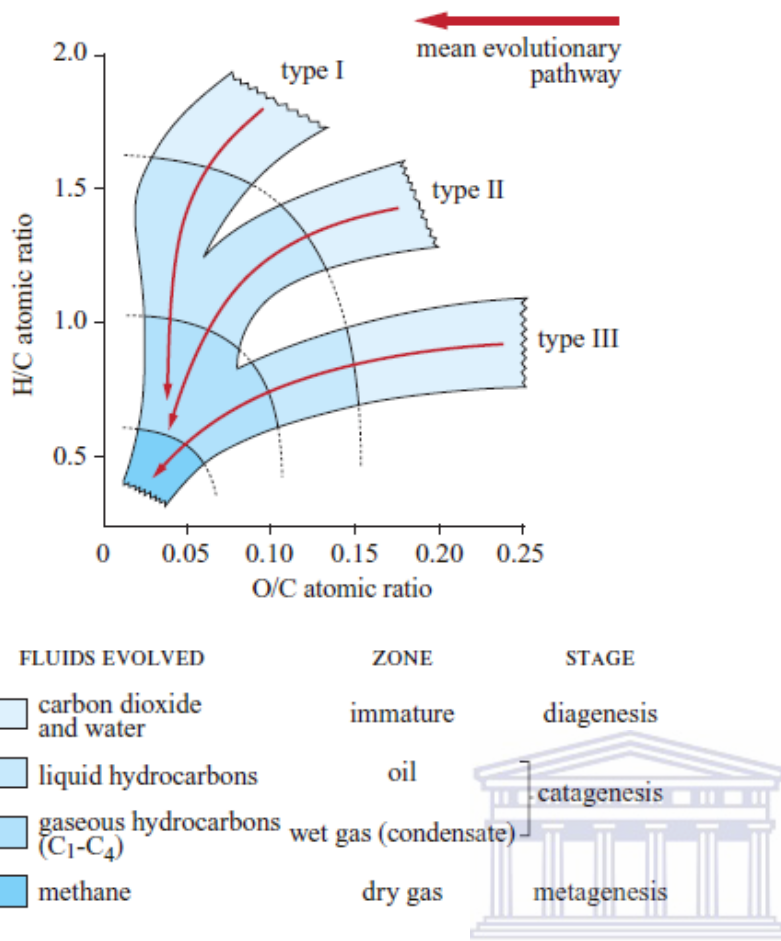


Figure 8. Classification of kerogens into three broad categories, expressed using the van Krevelen diagram. Elemental composition of organic matter in freshly deposited sediments plotted towards the upper right end of the field (diagenesis stage). With increasing burial, kerogen transformation proceeds during the catagenesis and metagenesis stages (Adapted from Killops and Killops, 1993 in Leythaeuser, n.d.).

3.2 Source rocks in the Bredasdorp Basin

Source rocks have been intersected in the Bredasdorp Basin during the drilling of wells. Davies, (1997) clearly highlights all the different source rocks encountered and divided the source into 7 categories based on the age of deposition.

3.2.1 Syn-rift source rocks (Late Jurassic)

These source rocks were deposited prior to the main marine incursion and are found at or near the base of the graben (Davies, 1997). These are lacustrine origin; with source rock potential varies widely from thin laminae of oil rich Type 1, oil prone source rocks to thicker beds of coarser, coaly shales and silts (Davies, 1997). They contain TOC contents varying from 1.1-2.7% of which a large

portion of the organic matter is amorphous and original HI of > 600 (Davies, 1997). The maturation levels recorded reached up 0.8% Vro. Davies, (1997) suggests that there is a pre-1At1 oil prone source rock due to the widespread presence of pyrobitumen.

3.2.2 Sequence 1A-4A Source rocks (Valanginian)

Wet gas to oil prone source rock is known to be present in these sequences, although it is likely that only one interval in these four sequences has source potential. In the south flank of the basin 1A-4A source rocks were encountered, because the sequences onlap basin margins and high away from structural crests (Davies, 1997). Deep topographic lows resulted in the basin after early Valanginian rifting; these lows were localised meaning there was low limited sediment provenance for some lows and sedimentation could have been largely pelagic (Davies, 1997). The TOC content is moderate, ranging from 1.0-1.5% and HI of ~ 400-500 (Davies, 1997).

3.2.3 Sequence 5A source rocks (Latest Hauterivian)

The base of this sequence contains a thin, locally oil prone source rock. Only a few wells intersect this interval thus showing minimum extent. The sediments were deposited in a restricted pelagic-hemi pelagic environment (Jungslager, 1996 in Davies, 1997), which is favourable for source rock development because organic matter preservation is more likely under dysoxic condition especially where restricted sedimentation occur (Demaison and Moore, 1980). The TOC content for these sediments is moderately rich with a high up to 1.8% TOC and HI averaging 200. The north flank of the basin has kerogen with quite high hydrogen content. The south flank has marginally oil prone source rocks, though they are very thin; these show very low maturity.

3.2.4 Sequence 6A-8A Source rocks (Early Barremian)

The source rock immediately above 6At1 is largely developed, as Horizon 6At1 is an angular unconformity (Davies, 1997). The 6A-8A source rocks distribution cluster in two distinct zones, the southeast and the north western part of the basin (Davies, 1997). These source rocks have TOC content ranging between 1.8-2.5%, and HI varying between 275 and 119. These are reported to be wet gas to oil prone source rocks.

3.2.5 Sequences 9A-12A source rocks (Late Barremian)

In the south flank and the western central parts of the basin, source rocks are found in the basal section of the 9A-12A sequences (Davies, 1997). They are reported to have been buried through the

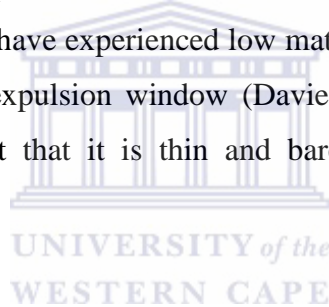
base of the oil window and into the top of the gas window (Vro 1.1 %) in different locations and are in the Type 2 region. The TOC content of these rocks range from 1.8-2.5%.

3.2.6 Sequence 13A source rocks (Early Aptian)

These source rocks are developed across most of the basin (Davies et al., 1988b and Brink et al., 1991 in Davies, 1997). They have considerable thickness and higher richness than any of the source rocks encountered, thus making them highly prospective. These formed in anoxic basin which organic material deposited in the core of the basin was dominated by oil prone material and rimmed by gas prone source rocks (Davies, 1997). The source rocks were found to be Type 2, with TOC contents significantly higher ranging up to 4.0% and HI ranging over 500 (Davies, 1997).

3.2.7 Sequence 15A source rocks (Early Turonian)

The source rocks in this interval are located at the eastern end of the basin (Davies, 1997). The sequence is thought to have been deposited in a sediment starvation model due to the known rate of deposition. It is however reported to have experienced low maturation levels, especially to the deeply buried rocks, which are in the oil expulsion window (Davies, 1997). It is not considered to be a significant potential due to the fact that it is thin and barely mature enough to generate large quantities of oil (Davies, 1997).



Chapter Four: Methodology

4.1 Database

4.1.1 Data

The study focuses on the maturity of the syn- and post-rift source rocks of the Bredasdorp Basin. Various data sets were utilised, and these include Twelve (12) 2D seismic sections and well data. Well data comprises well logs, formation tops, check-shot, borehole temperature as well as geochemical well data i.e. vitrinite reflectance data. Achieving this level of data integration, the model was able to demonstrate likely maturity conditions of the syn- and post-rift source rocks of the Bredasdorp Basin.

Table 1. Data that was used to conduct the research project.

Data	
Well Reports	
Geological report	SCAL
Geochemical report	Biostratigraphy
Conventional core analysis	
Wells (LAS Format)	
F-O1	F-R1
F-O2	F-S1
Seismic Sections	
12 Seismic sections	
Logs	
Gamma ray	Density
Resistivity	Neutron
Sonic	
Core data	
Porosity	Permeability
Other data	
Temperature	Check shots
Pressure	Well tops
Vitrinite reflectance	

4.1.2 Data Summary

1. Well Data

The four wells were used in the study and these were selected because they intersected the seismic sections used in the project (Figure. 9). Using well tops data and the gamma ray log, different zones were created (Figure. 10). It is evident that some of the zones were completely eroded in some wells, like in the case of 1At1 which is present in all the wells except in F-R1 (Figure. 10).

Table 2. General well information.

Well Name	X Coordinate	Y Coordinate	KB	Depth (m)
F-O1	639384	6109718	26	3914
F-O2	642088	6112852	25	3891
F-R1	645784	6108655	22	4562
F-S1	654485	6108394	30	3950

2. Seismic Data

2D seismic sections were selected in a north-south (short axes) and east-west (long axes) direction creating a grid network covering the study area (Figure. 9). A list of the seismic sections used is listed below (Table. 3).

Table 3. List of seismic sections used in the study.

Seismic Lines	
N-S Lines	E-W
F90 – 148	F91 – 231
F90 – 149	F93 – 217
F90 – 150	F93 – 218
F93 - 210	F93 – 220
F93 – 211	
F93 – 213	
F93 – 203	
F93 – 201	

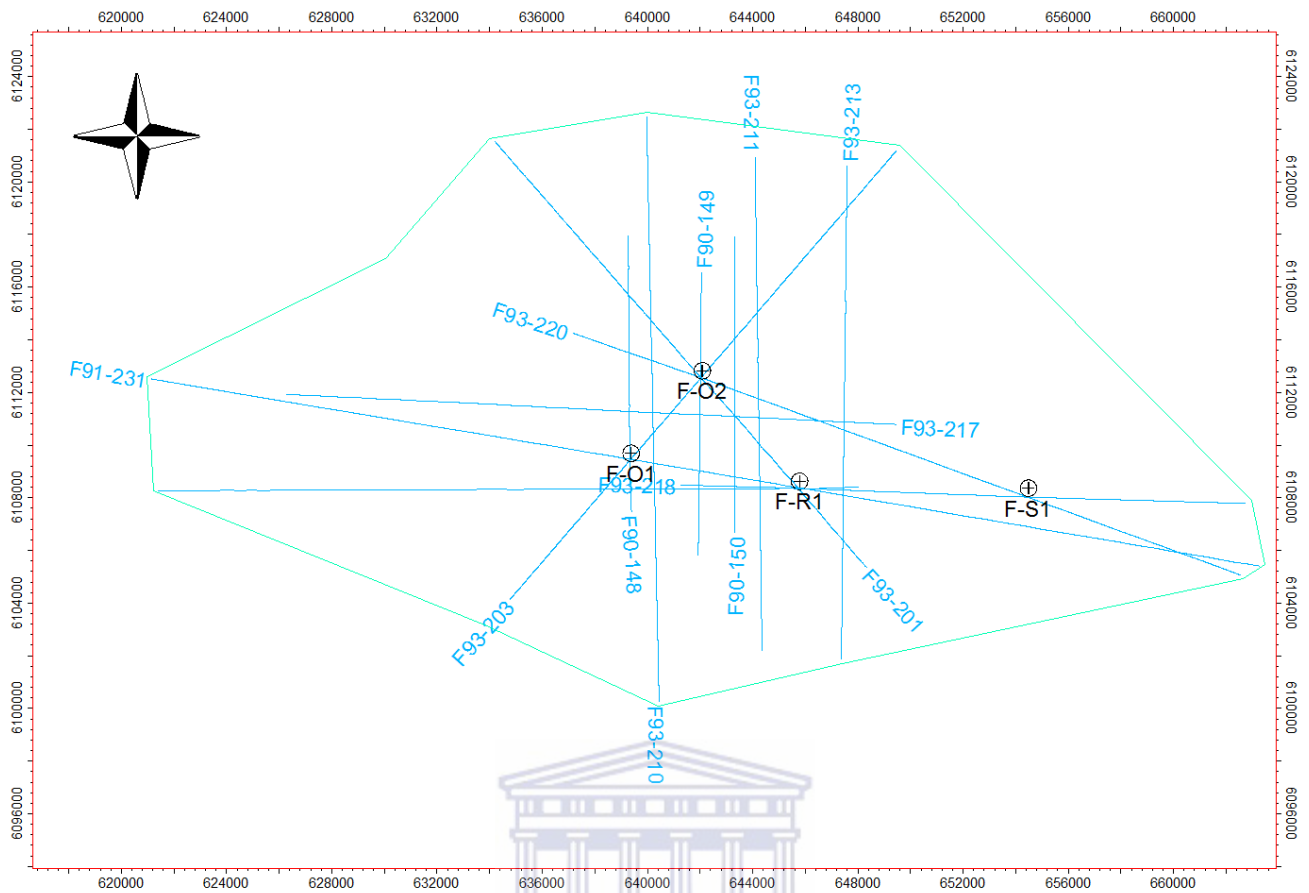


Figure 9. The spatial relationship of the wells and seismic sections within the outlined study area.

4.2 Research Workflow

4.2.1 Seismic interpretation and Velocity modelling

This section was achieved with the use of Petrel software, which is used in the exploration and production sector of the petroleum industry. Using 2D sections and well data (well tops and well logs), seismic to well tie was performed to correct for mis-ties through bulk shifting. Major unconformities were then interpreted based on the position of the well tops data (Figure. 11), to create horizon surfaces over the study area through interpolation between seismic interpretations for all the interpreted unconformities and seafloor. Velocity model was created with the use of checkshot data. These surfaces were depth converted using the interval velocities, from the velocity model created. The resulted surfaces were exported to PetroMod for building the 3D model.

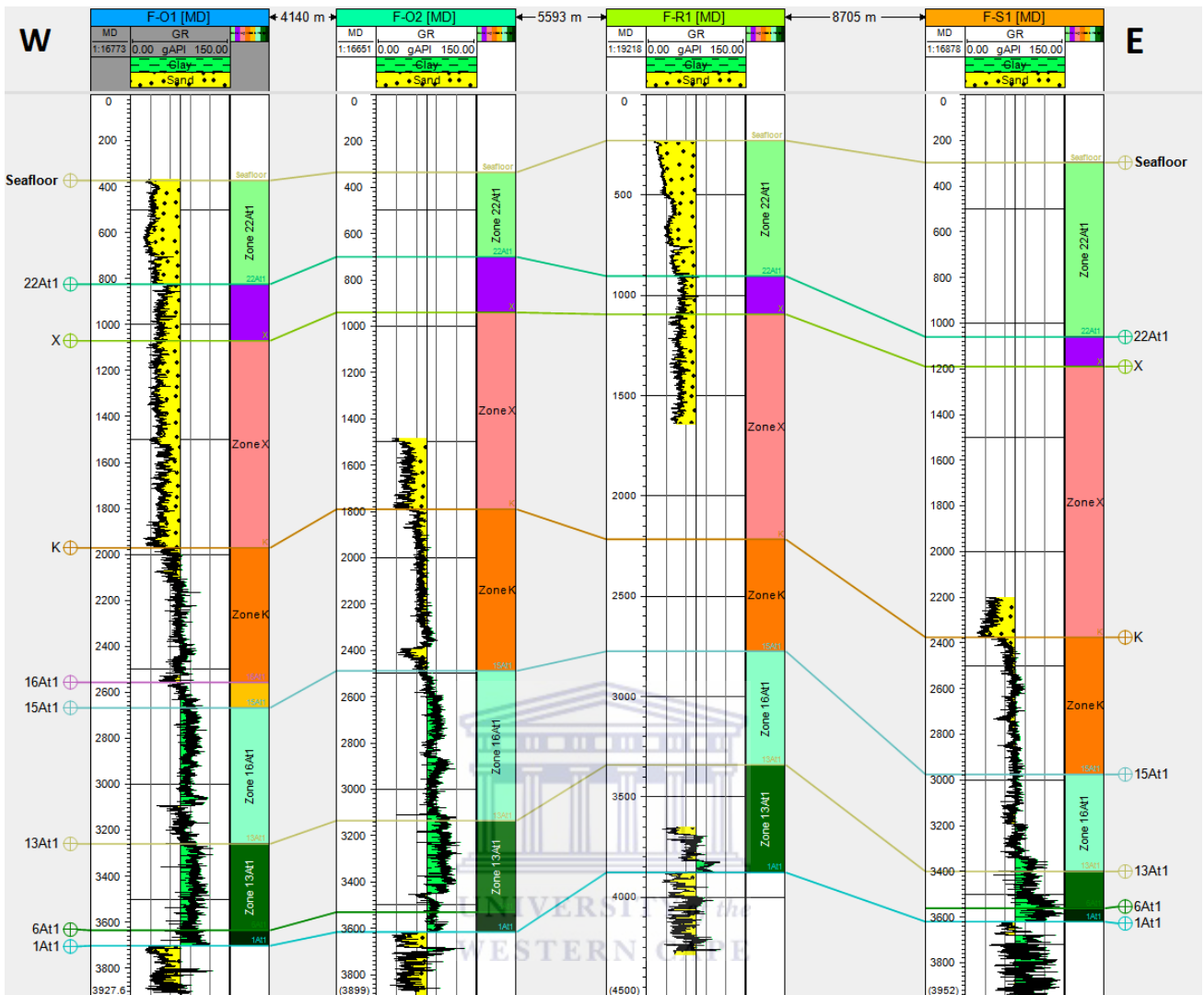


Figure 10. W-E well correlation panel showing different zones based on the combination of gamma ray log and well tops.

4.2.2 3D Model building and simulation

Data used in this modelling were obtained primarily from well data and exported surfaces from Petrel. The model was built using the Petrobuilder module in Petromod. The most important building blocks used in this 3D modelling are the depth maps of the F-O gas Field which were imported into Petrobuilder. In this work, a simple basic model is built first before proceeding to apply erosion to the model. The lithofacies of the various formation and the petroleum system elements are defined in the facies definition table. Seventeen layers have been defined in the age assignment table as compared to 13 lithofacies in the facies definition table because one or more layers can have the same lithofacies. The petroleum system elements in the basin such as source rock, reservoir and seal are also defined. The migration method used to simulate the model is generation only method in Petromod, which basically simulates the generation of the hydrocarbons.

1. Age Assignment

One of the core aims of basin modelling is to build a model which can be simulated from the start of deposition to present day. Therefore, one of the most important aspects of building a model is the assigning of stratigraphic ages. This is done in the age assignment table in Petromod. Erosions magnitudes are also defined in the age assignment table. To define erosion, data on the age of the erosion and the thickness eroded is needed. In the Bredasdorp Basin, three episodes of erosion occurred and these are clearly defined in the model. These episodes occurred in, early Cretaceous (140-135 Ma), Eocene (43-38 Ma) and late Miocene (16-11 Ma) (Sonibare, subm.).

2. Paleo-geometries

Boundary conditions define the basic energetic conditions for temperature and burial history of the source rock and, consequently, for the maturation of organic matter through time (Sonibare, subm.). Three main boundary conditions need to be defined in basin modelling namely Heat Flow (HF), Paleo Water Depth (PWD) and Sediment Water Interface Temperature (SWIT). The HF trend first needs to be created and then assigned to the model. Heat flow determines the maturity of the source rock. Heat flow values have been defined and assigned to the model from 0 Ma (60 Mw/m²) to 125 Ma, (75 Mw/m²) to 157 Ma (75 Mw/m²). The sediment-water interface (SWIT) is defined using the automatic function in Petromod. At the upper boundary corresponding to the present-day seafloor, we defined the sediment-water interface temperature (SWIT) through time following the approach of Wygrala, (1989) incorporating paleo-latitude variations for our study locality. The hemisphere is defined as southern and the latitude as 34. The assigned surface temperature gives a present-day SWIT as warm as 18 °C, which corresponds well with the seafloor temperature described by Goutorbe et al., (2008).

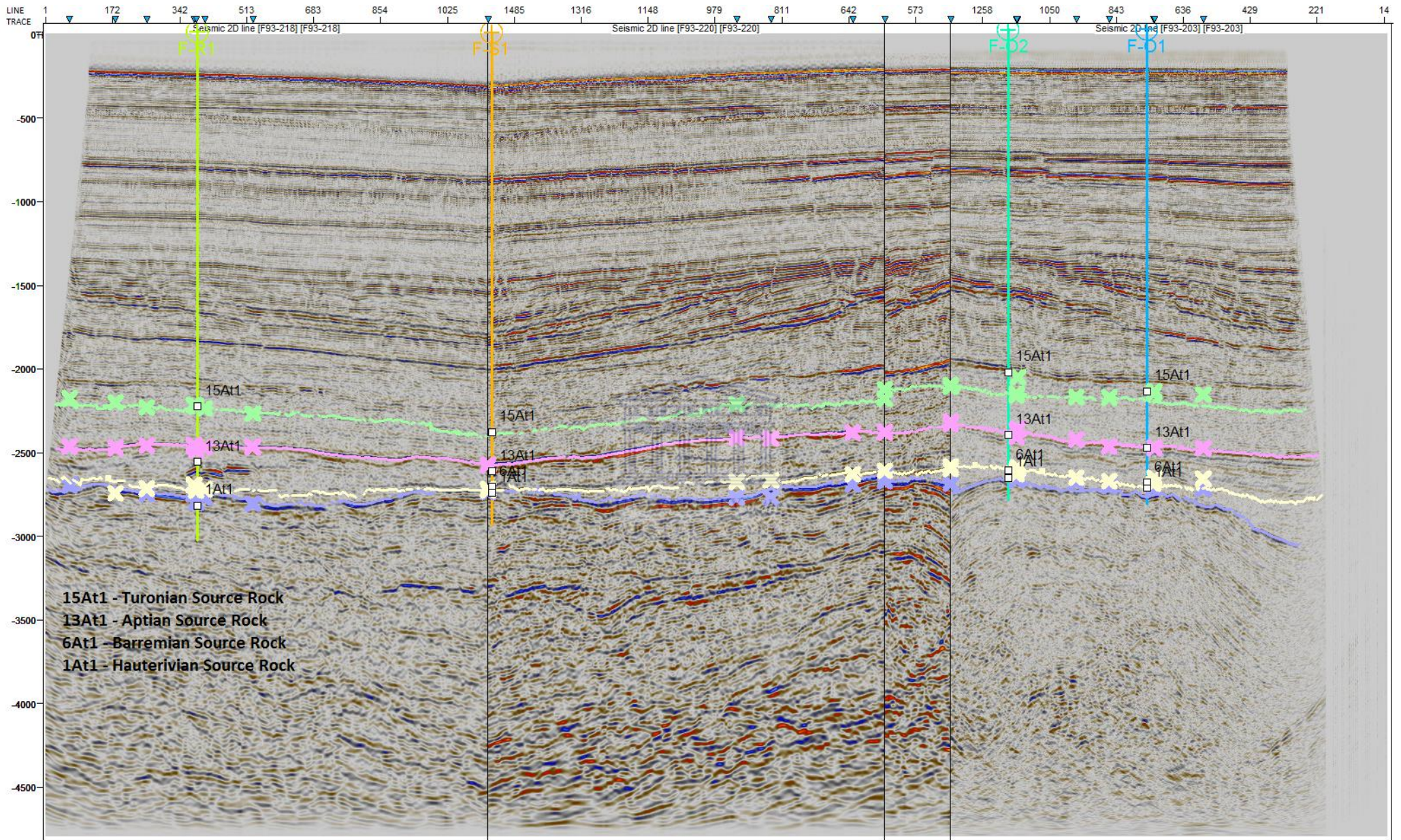


Figure 11. Seismic composite line showing all the wells and the position of the source rocks in the F-O Gas field.

3. Source rocks and their assigned parameters

Intersected shale dominated intervals in all the wells indicate the presence of Lower to Upper Cretaceous source rocks containing 1.5 to 3 % total organic carbon (TOC) within the syn-rift and post rift sediments in the Bredasdorp Basin. Four source rocks were identified and are similar to the source rocks identified in the Bredasdorp Basin. These were considered in the study and used for organic matter maturation and petroleum generation. The four source rocks used relate to one syn-rift source rock Hauterivian (Organic rich shale), and three post-rift source rocks, namely: Barremian (Organic rich shale), Aptian (Organic rich with TOC 3%) and Turonian (Organic rich shale). The source rocks locations are clearly marked out in the seismic section profile (Figure. 11) and the parameters allocated are shown in Table. 4. These parameters were defined based on the source rock properties for the available wells in the gas field.

TOC and HI were allocated as average values to each source rock interval at respective modelled well locations. Of all the modelled source rock intervals, the Aptian source rock records the best source potential consisting of Type II kerogen with 3 % TOC and HI of 400 mgHC/gTOC. The kinetics group, "Burnham (1989)-TII", after Burnham (1989), was selected in Petromod to determine the timing of oil and gas generation. This group is deemed suitable for source rocks with Type II kerogen as it leads to the generation of both oil and gas in the model results. The maturation history was modelled based on the "EASY [%Ro]" method of Sweeney and Burnham, (1990). The ranges of 0.55, 0.7 and 1.3 %Ro values have been selected to represent the start, peak and end of oil generation, respectively.

Where scarce data is recorded for any source interval particularly for the Hauterivian and Turonian source rocks, we constrained this limitation by integrating source rock information from the studies of Sonibare et al., (subm.). The work flow development for the study is indicated in Figure. 12.

Table 4. Input parameters for the modelled source rocks intervals in the 3D model.

Source Rock Interval	Kerogen Type	Thickness [m]	TOC Value [%]	HI Value [mgHC/gTOC]	Kinetics
Hauterivian	II/III	30 - 50	1.7	220	Burnham (1989)_ TII
Barremian	II/III	15 - 30	1.8	205	Burnham (1989)_ TII
Aptian	II	57 - 70	3	400	Burnham (1989)_ TII
Turonian	II/III	10 - 20	1.5	135	Burnham (1989)_ TII

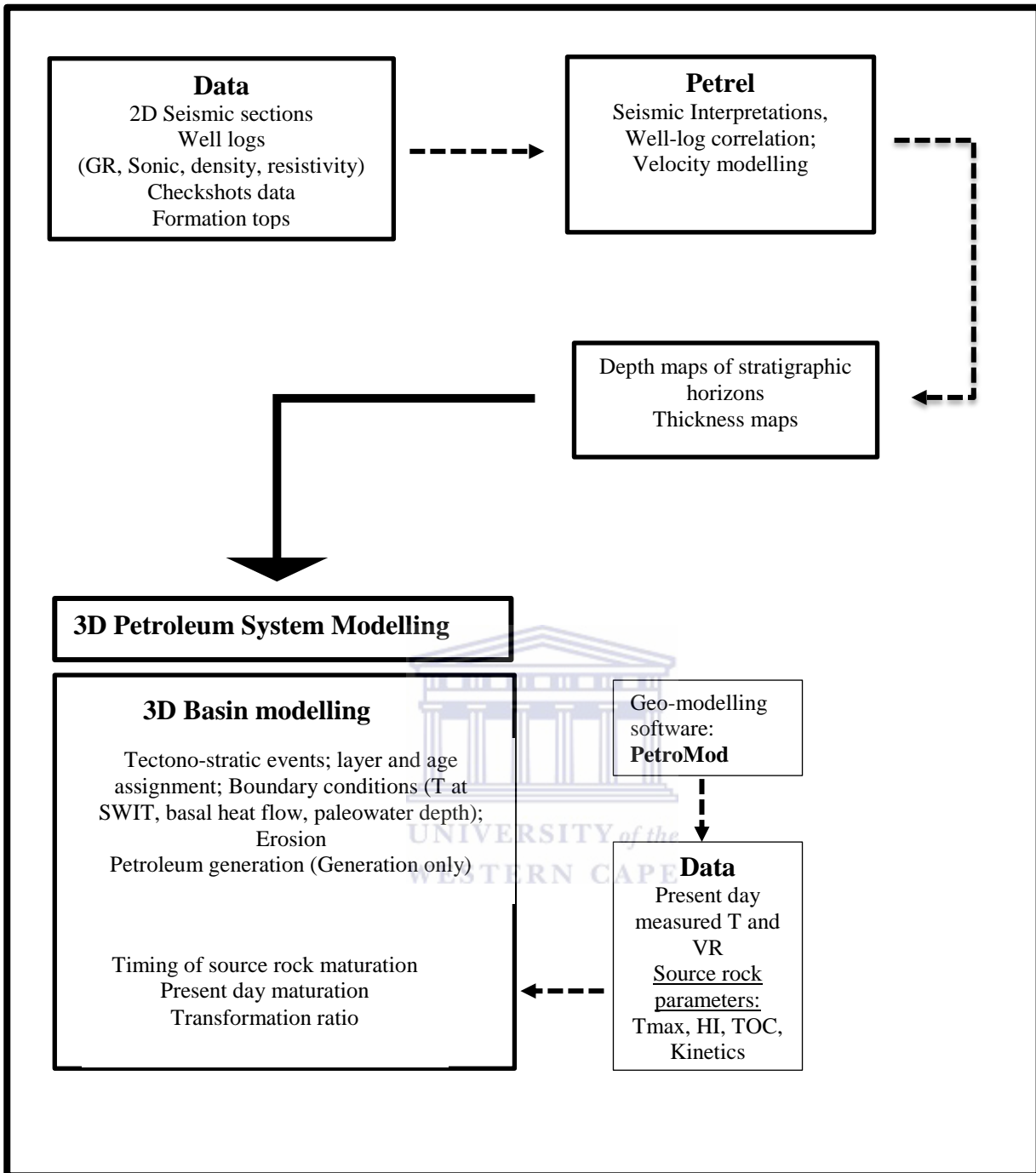


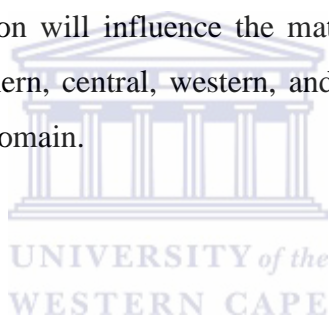
Figure 12. Integrated workflow developed for the study.

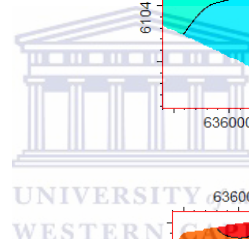
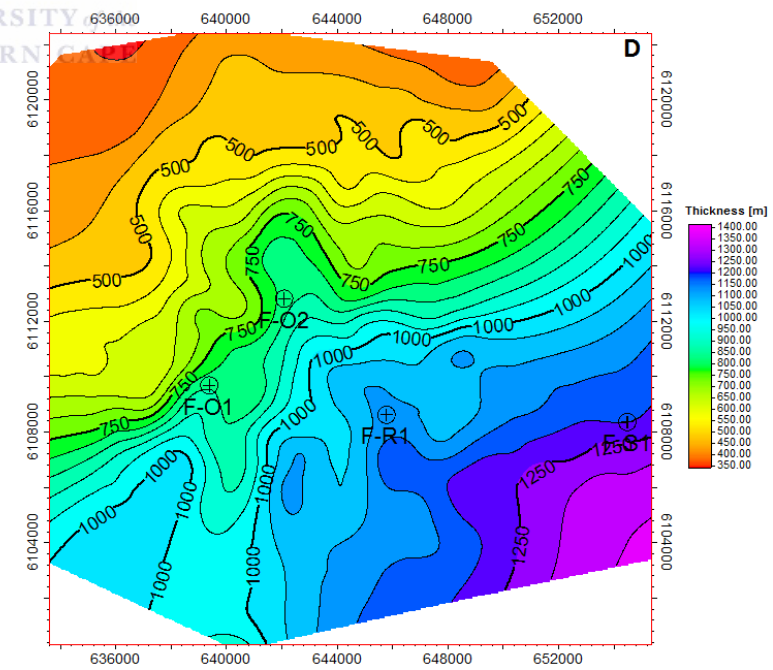
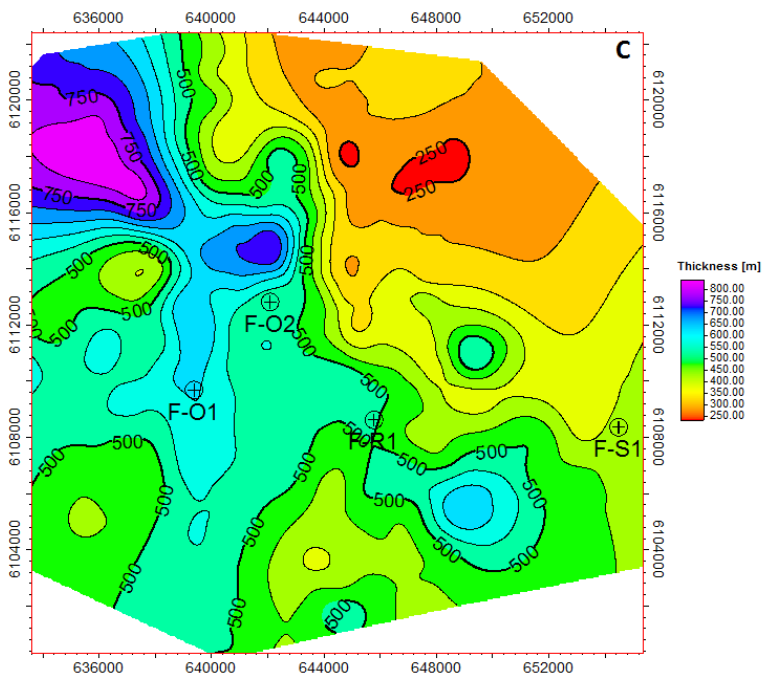
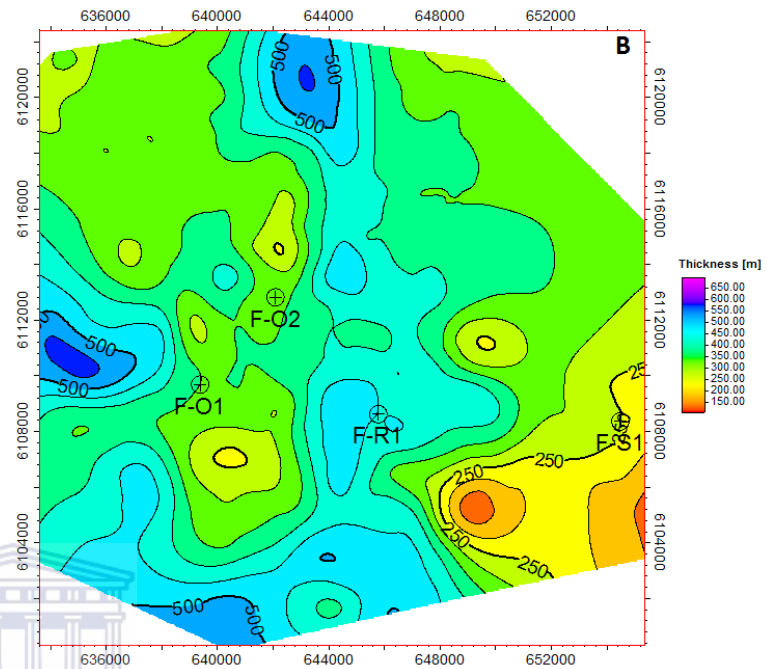
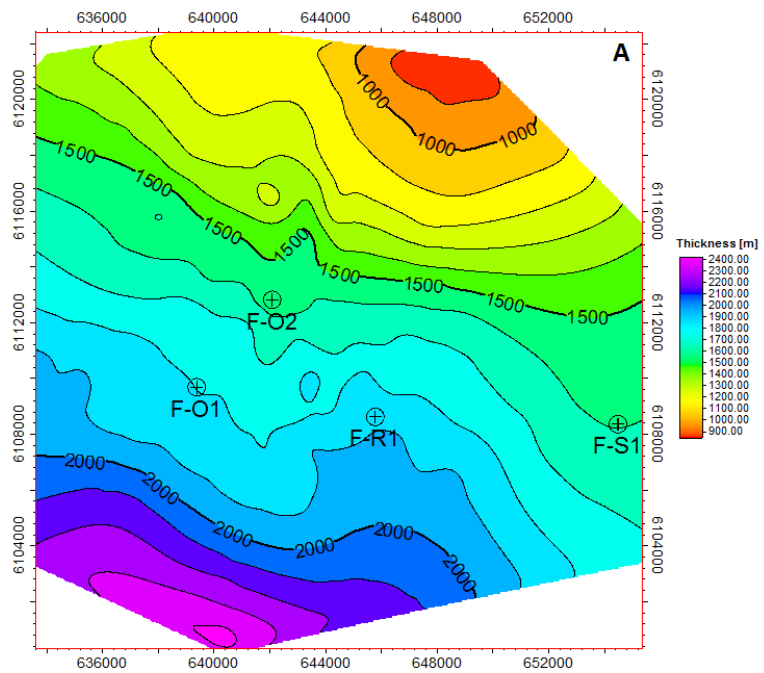
Chapter Five: Results and Discussion

5.1 Source Rock Maturation

5.1.1 Thickness Maps

The 3D model shows the robust insights into the present day structure. The sedimentary infill of the model is structurally characterised by basin-wide unconformities (Figure. 13 A-D). The 1At1 unconformity illustrates that thicker sediments are mostly in the southern domain than in the northern domain (Figure. 13A) attaining up to 2400 m in thickness. 13At1 and 17At1 unconformities show also thicker sediments in the southern and western domains (Figure. 13 B&C). The 17At1 unconformity shows that sediments are thicker on the eastern and the southern domains with sediments attaining a thickness of up to 1400 m. The North-South 2D cross section (Figure. 13E) is also attesting to this fact that the southern domain contains much thicker sediments than the northern. This overburden thickness distribution will influence the maturation of source rocks in the study area, thereby ensuring that the southern, central, western, and eastern domains will probably have higher maturation than the northern domain.





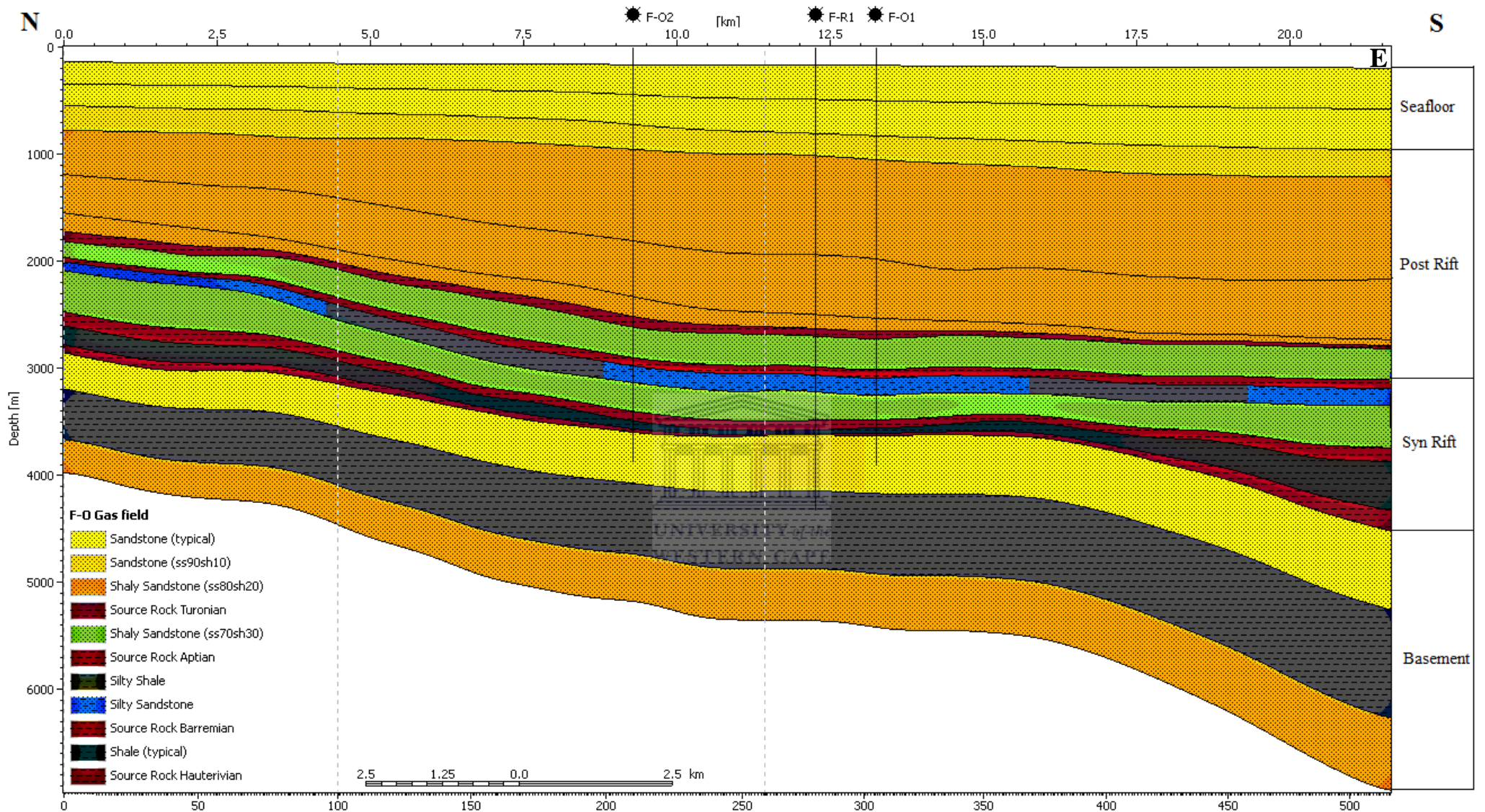


Figure 13. Thickness maps of the major unconformities (A) 1At1; (B) 13At1; (C) 15At1; (D) 17At1. (E) North-South cross-sectional profile through the consistent 3D structural model of the F-O Gas Field indicating the modelled 17 layers with their according vertical and lateral lithofacies distribution and areal distribution of potential source rocks.

5.1.2 Thermal calibration

The model was calibrated using two of the major controllers of maturity, heat flow and amount of sediments eroded. As such, calibration was done using vitrinite reflectance (VRo), Rock-Eval maximum temperature (Tmax) and Bottom Hole Temperature (BHT).

This thesis assumed a simple rift model characterised initially with high heat flow corresponding with the rifting event which began from 157- 131 Ma. This was then followed by constant heat flow which is linked to the post rift event. For the initial rifting event, a higher heat flow value was assigned, while post rift event was assigned a constant value (Figure. 14). Major erosional events that occurred and were included in the model include: Lower Cretaceous (140-135 Ma), Paleogene (43-38 Ma), and Late Miocene (16-11 Ma). The Late Miocene has the largest magnitude with sediments 600-720 m thick eroded. These episodes were included in the modelling since the effects of uplift and/or erosion throughout are considered to have major impact on the present-day maturity and temperature trends (Figure. 15).

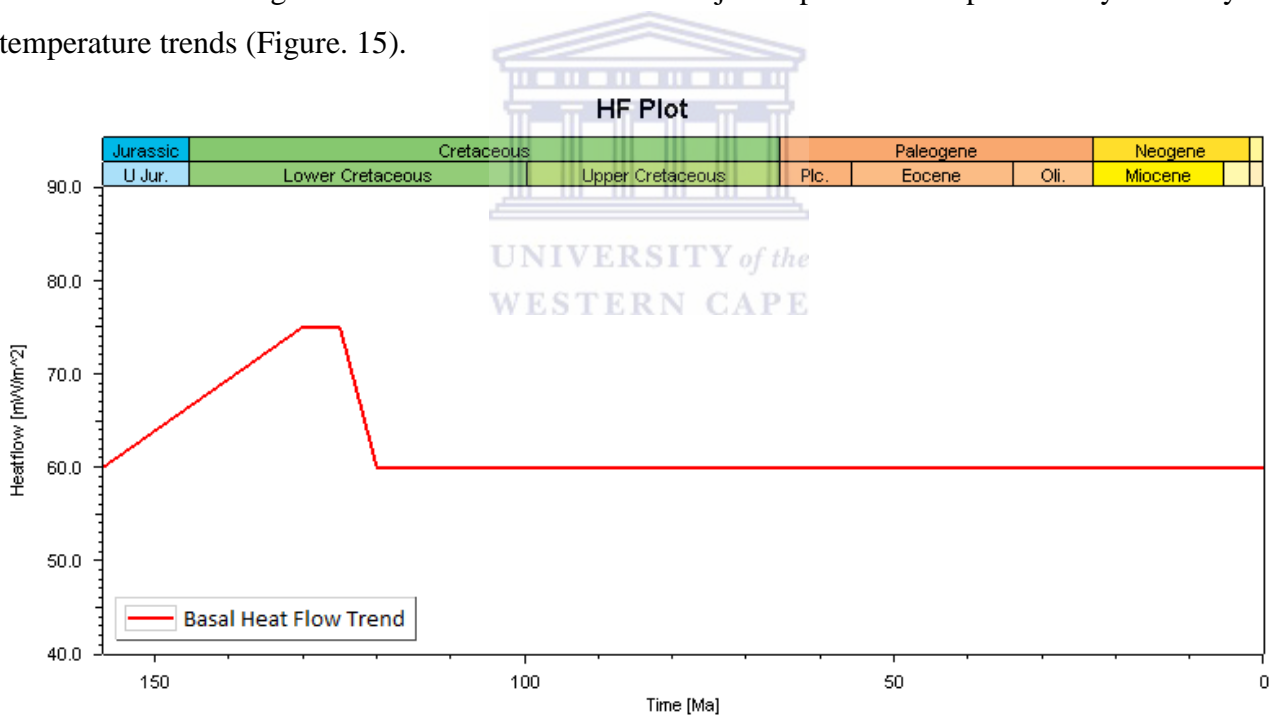


Figure 14. Basal heat flow trend over time.

5.1.3 Burial and thermal plots

The constructed burial and temperature histories of the studied wells are shown in Figure. 15A–D. Reconstruction of burial history indicates a steep subsidence and sedimentation during the Early Cretaceous and a relatively steady subsidence in Paleogene for the study area. Steep subsidence is indicated by major tectonic events before the main phase of continental breakup. Burial histories for

all the studied wells are approximately similar in that they contain three major erosional events. In order to investigate the accuracy of the calibrated thermal and maturity models, the thickness of overburden, timing and duration of hiatus and surface erosion intensity were all considered. The results for each of the studied wells, the best fit models were picked, whose results are presented here.

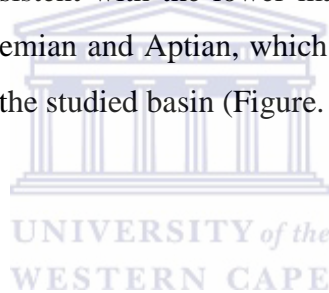
1. F-O1 Well

Figure 15A displays a burial history diagram of the F-O1 well. Formation temperature data were estimated based on bottom-hole temperature. This well exhibits a continuous burial and sedimentation throughout most of its history (since Upper Jurassic to Seafloor sandstone) which led to deeper burial depths resulting in the maturity of the source rocks in the well. Rapid subsidence occurred in 140 Ma, which was due to the concurrent rifting and sediment deposition. The rapid burial was short lived and followed by rapid uplift which ended approximately 130 Ma. In the period 90-80 Ma, rapid burial occurred and was followed by a short period of stagnation. Burial resumed until 44 Ma until short period of uplift occurred with subsequent erosion in Eocene and Miocene. Based on a detailed inspection of a combination of seismic, stratigraphic and well log data, it is suggested that over 420-440 m and 220-260 m thick sediments were eroded from the Paleogene and Cretaceous respectively. With a total drilled depth of 3952 m, the maximum burial temperature for the well is estimated between 116 and 156 °C and the calculated vitrinite reflectance values range from 0.5 to 2.0 % VRo (Figure. 15A). This shows that the source rocks are in the oil generation window with possibility of some oil converted to gas. The Hauterivian which is the oldest experienced deeper burials, thus higher temperatures (150 °C) which led to maturation as indicated by the vitrinite plot (Figure. 15A). With this increased temperatures, this indicates that the Hauterivian is in the late stage of oil generation window and may have converted some of the oil to gas. The Barremian source rock recorded vitrinite reflectance values of 0.55-1.0 % VRo; an indication that it is moving from early oil to the main oil window. The Aptian has been buried to depths up to 3259 m where it is in the late oil with some oil converted to gas (Figure. 15A). The Turonian source rock which is in shallower depths as compared to the other three source rocks shows that is in the early oil window, as indicated in Figure. 15A.

2. F-O2 Well

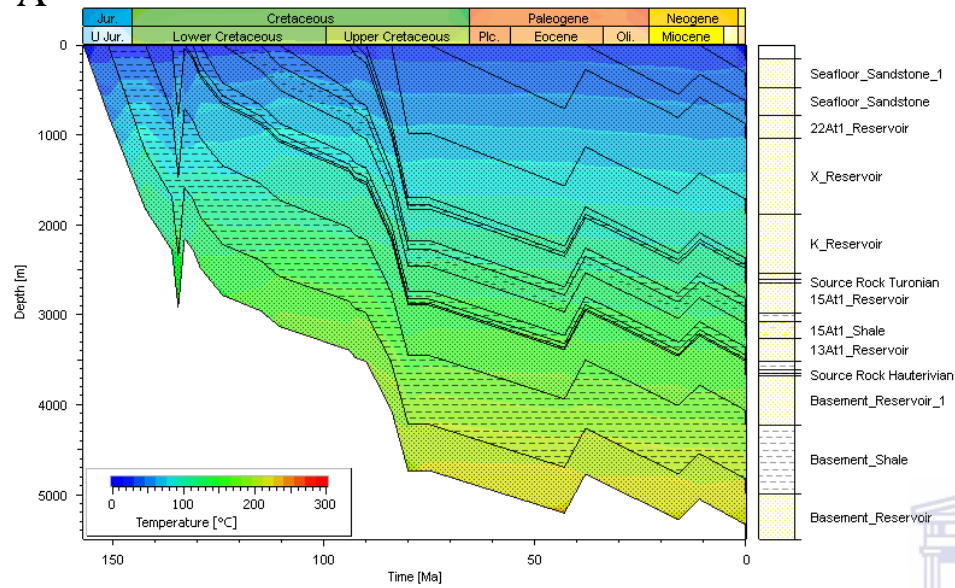
An approximate thickness of 3899 m has been drilled in this well and its maximum burial temperature varies with maximum temperatures encountered to be reaching 164 °C (Figure. 15B).

The F-O2 well like the F-O1 also experienced fast burial periods until it stopped due to rapid uplift and thus erosion approximately 140 Ma (Figure. 15B). This period was then followed by rapid subsidence until 43-36 Ma and 16-11 Ma, where uplift with subsequent erosion occurred. Measured bottom-hole temperatures suggest a present-day gradient of about 41.3 °C/km. Both the temperature and vitrinite reflectance trends (Figure. 15B) have a reasonably good fit with the observed data. Measured vitrinite data were available for the Barremian, Aptian and Turonian source rock. With vitrinite values ranging 0.50 – 1.5 % VRo, the source rocks are in the early oil to late oil generation stage of the oil generation window. The Hauterivian and Barremian source rocks are interpreted to be within the late stage of oil generation window, as indicated by calculated vitrinite reflectance values of 1.35% VRo and maximum burial temperatures of 130–140 °C (Figure. 15B). The Aptian source rock is found also to be in the late oil stage with vitrinite values of 1.1% VRo as well as temperature of 115 °C (Figure. 15B). Turonian source rock, in comparison, shows a calculated vitrinite reflectance value of 0.7– 0.75% VRo and a maximum burial temperature of 80–85 °C (Figure. 15B). These results are consistent with the lower maturation of the Turonian source rock compared with the Hauterivian, Barremian and Aptian, which is also supported by the younger age and shallower burial of the former in the studied basin (Figure. 15A-D).

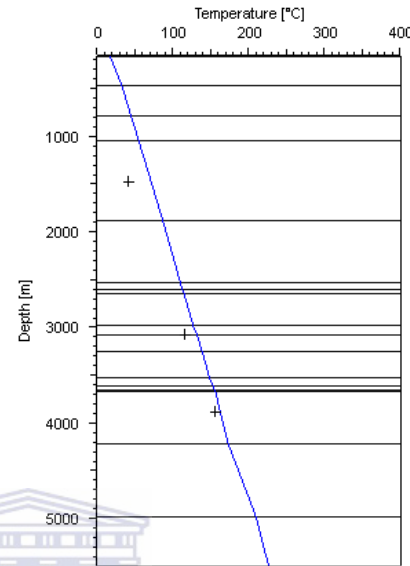


A

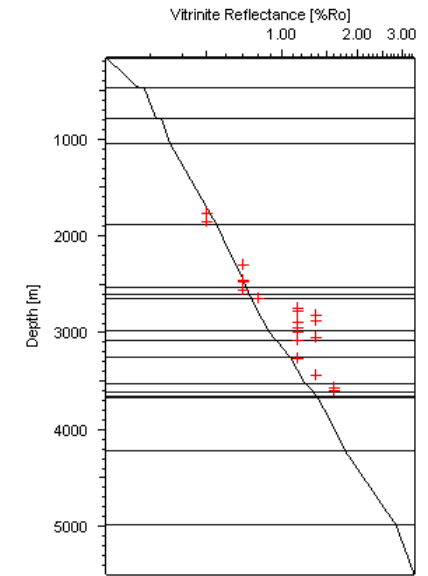
Burial and Temperature Plot at Well F-01



Temperature at Well F-01

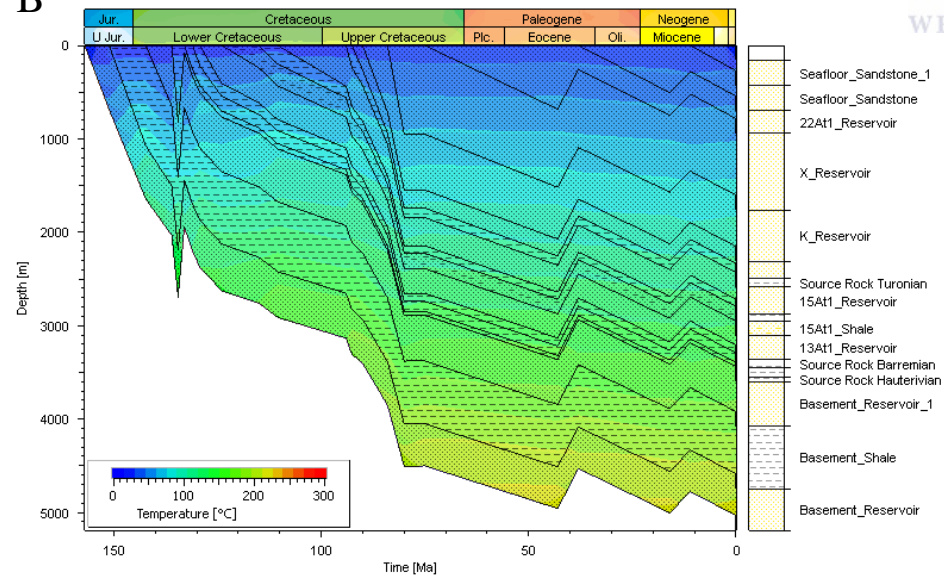


Vitrinite Plot at Well F-01

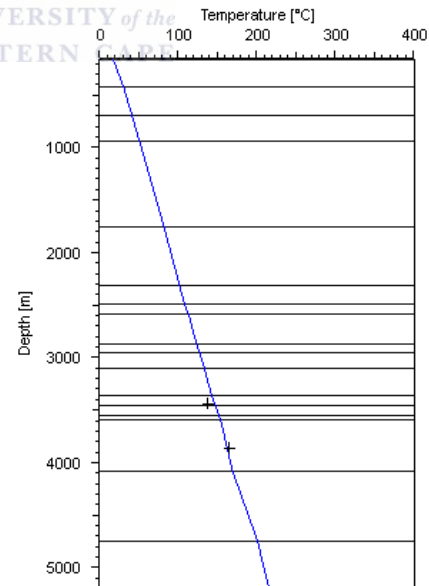


B

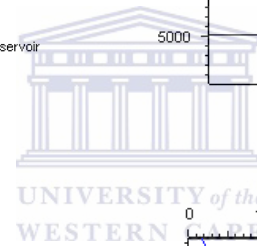
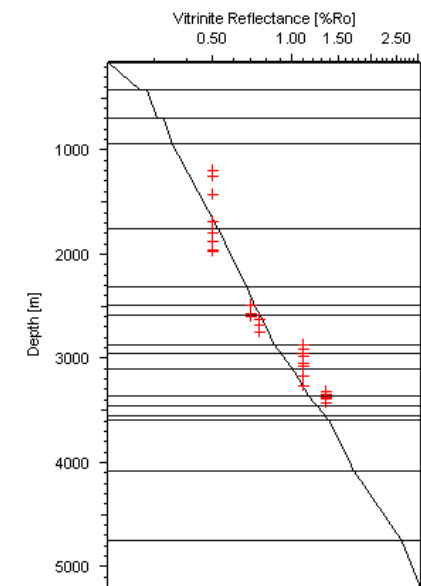
Burial and Temperature Plot at Well F-02



Temperature at Well F-02



Vitrinite Plot at Well F-02



UNIVERSITY of the WESTERN AUSTRALIA

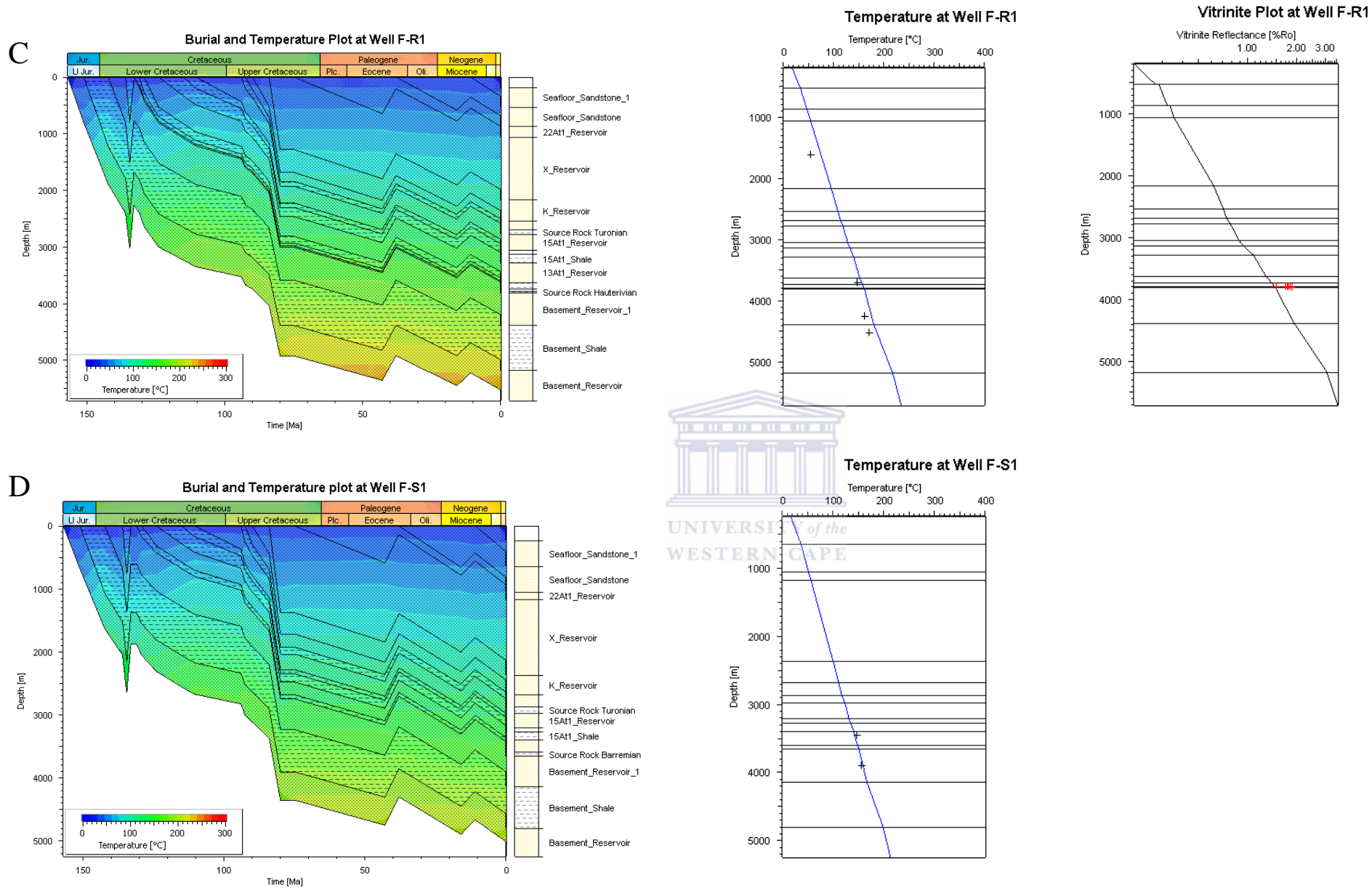


Figure 15. Burial history with temperature overlay and cross plot of measured and modelled temperature and vitrinite reflectance at wells: F-O1 (A), F-O2 (B), F-R1 (C) and F-S1 (D). Solid line = modelled; Plus sign = measured. Note F-S1 has no measured VR.

Burial and Temperature Plot at Well Pseudo North

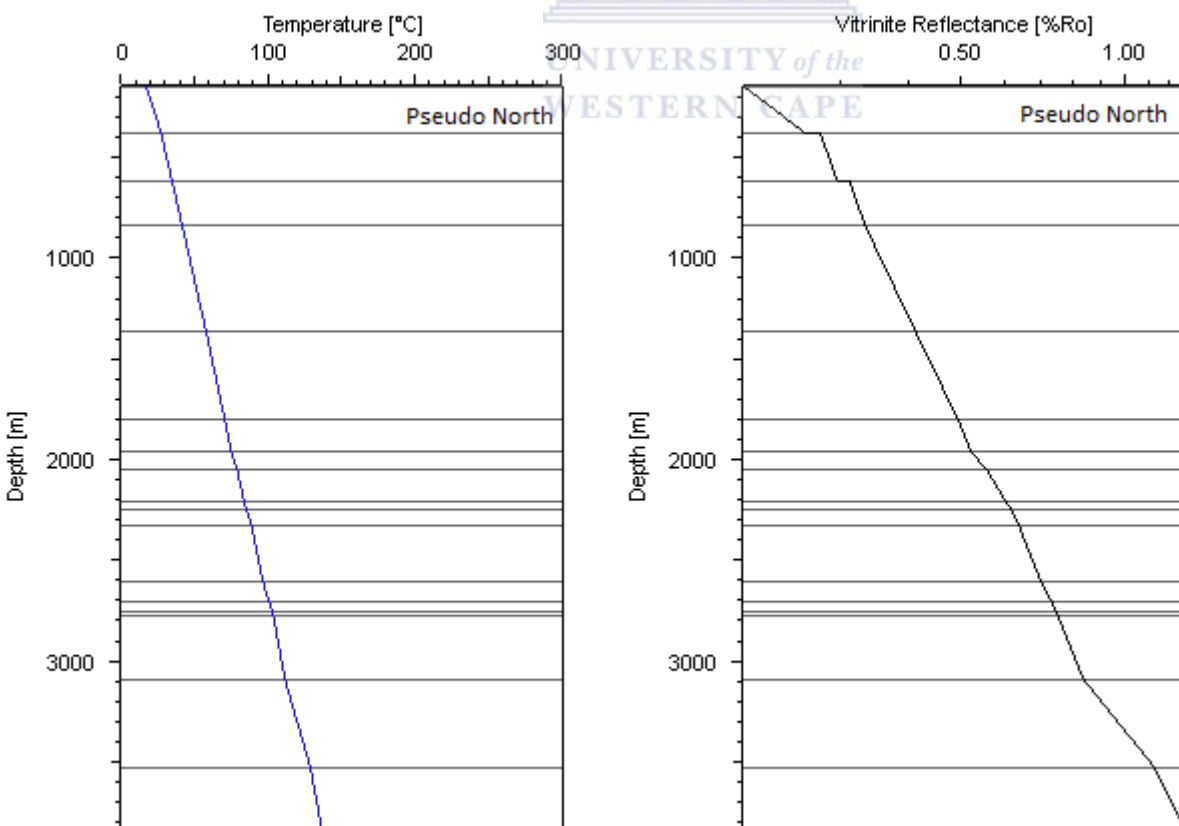
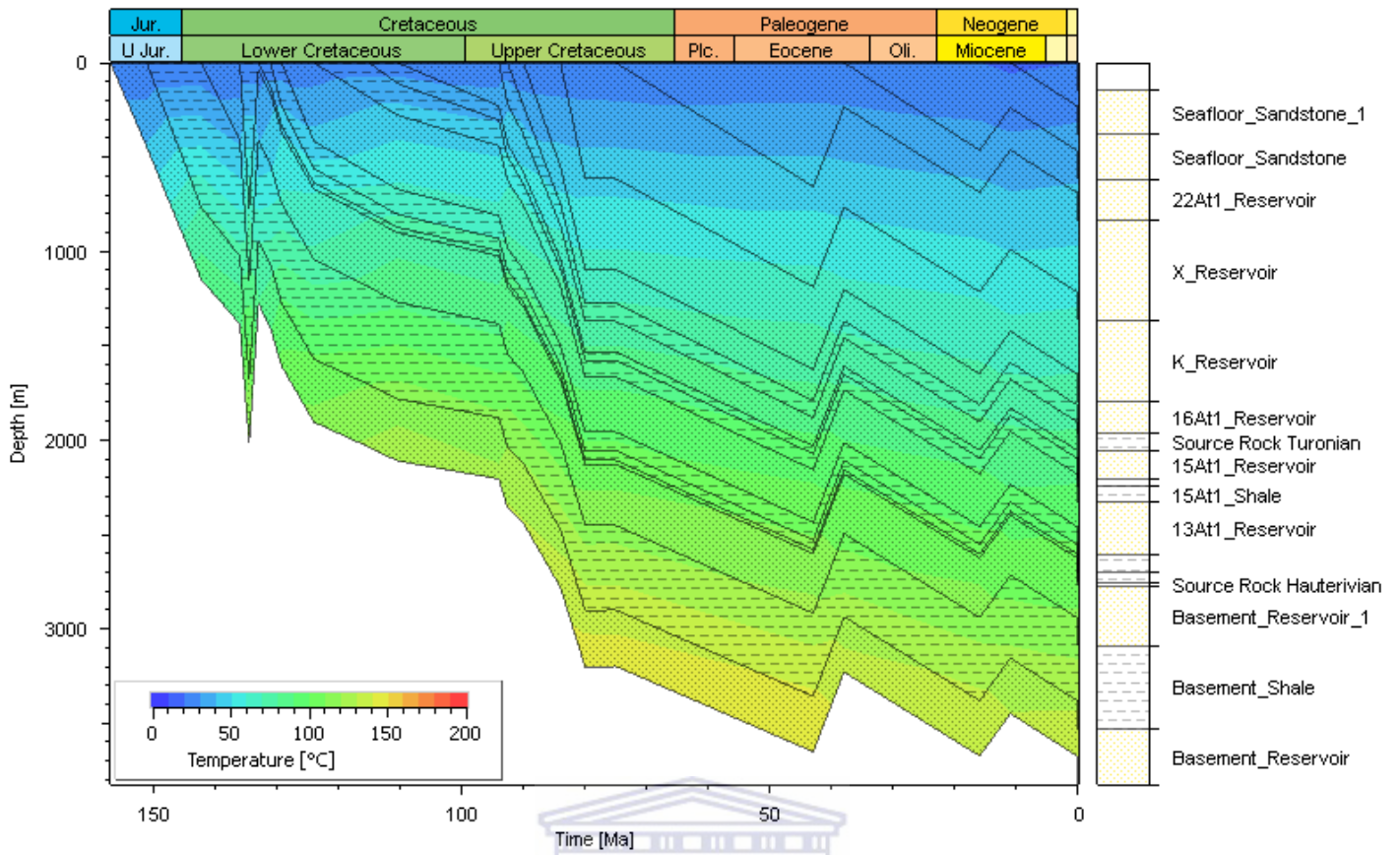


Figure 16. Burial history with temperature overlay and cross plot of modelled temperature and vitrinite reflectance at well Pseudo North. Solid line = modelled. Note no measured temperature and vitrinite reflectance.

3. F-R1 Well

The F-R1 well is the deepest well in the studied area, which penetrates portions of the pre-1At1 sediments with a total drilled depth of 4500 m (Figure. 15C). The measured bottom-hole temperature values imply a present-day geothermal gradient of 35.5 °C/km for F-R1 well. Based on burial history diagrams, the maximum burial temperature measured within this well is 170 °C for the pre-1At1 sediments (Figure. 15C). Vitrinite reflectance values ranging between 1.5-1.9% VRo were measured from the Hauterivian source rock, an indication that the Hauterivian source rock has passed the late oil generation stage and converted some of the oil to gas. It is noteworthy that the Hauterivian source rock attains a thickness of 3910 m in this well, which is much deeper than in the other wells. The Barremian source rock has temperature of about 146 °C; an indication that this source rock is in the late oil window. In contrast, the Aptian source rock in the burial history model have burial temperatures ranging from 110 to 120 °C and are presently in the main oil generation window (roughly at 0.7–1.0% VRo) (Figure. 15A&B). Compared with other wells, the Turonian source rock has reached levels of maturity in the early oil window.

4. F-S1 Well

The F-S1 is in the eastern most part of the modelled area. The stratigraphic sequences within this well are much thinner than in other three wells, the sequence actually thickens towards the western part of the model area. Like the other three wells the F-S1 experienced a similar burial history trend. The Hauterivian source rock is absent in this well, due to uplift and subsequent erosion (Figure. 15A-D). The Barremian source rock thus lies on the 1At1 unconformity, the burial depths of this source rock reached 3561 m, with temperatures reaching 140 °C (Figure. 15D). This shows that the source rock is in the main oil generation window, where estimated vitrinite values are in the ranges of 0.70–1.0% VRo (Figure. 15B). The Aptian source rock on the other hand is buried to depths with temperatures reaching 120-130 °C, an indication of the main oil window generation window (Figure. 15D). The Turonian source rock has temperatures up to 110 °C an indication that the source rock has gone through some transformation.

5. Pseudo North Well

The Pseudo North well was extracted from the northern domain of the modelled area, where there are no wells drilled. From the burial diagram it is noteworthy that this is the shallow part of the model area, with sediments attaining only 3800 m in thickness (Figure. 15). Modelled temperatures

are relatively low compared to those in other wells. The vitrinite reflectance plot shows that the source rock is mainly in the early oil while some areas are immature (Figure. 15).

5.1.4 Transformation ratio and maturity

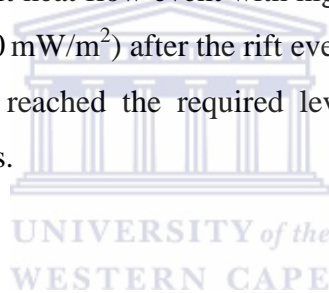
Among the results of PetroMod modelling are time-lapse maps of the transformation ratio, or percentage of kerogen transformed into petroleum, for each source rock (Figure. 17A-H). In general, as burial depth increases, more of the source rock passes through the oil-generation window, allowing more complete maturation of the organic matter. The time extraction of the older Hauterivian, Barremian, Aptian and the Turonian source rock at different well locations aims to portray the timing of maturation of the source rock at various locations within the basin. The transformation ratio in each source rock shows that they have undergone some degree of kerogen transformation. The older source rocks (Hauterivian and Barremian) have attained higher transformation ratio of up to 100 % with some exception at the northern domain (Figure. 17 A&C).

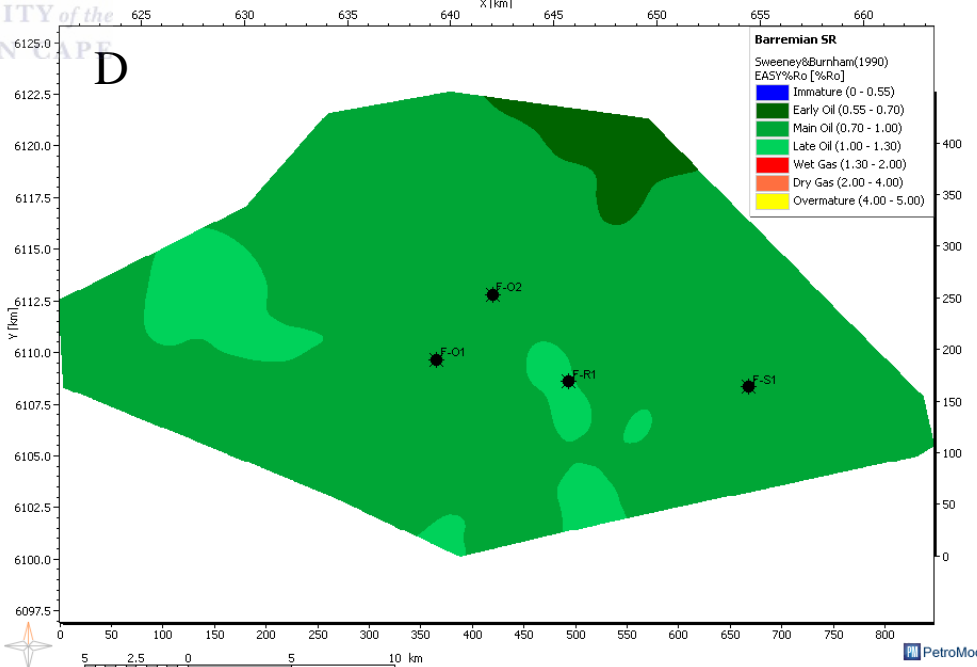
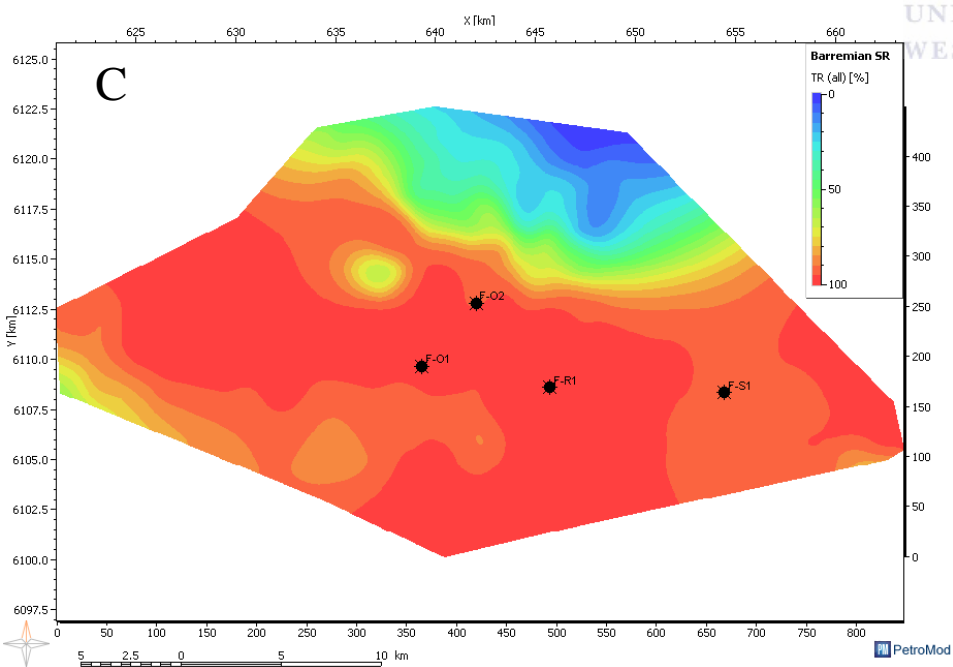
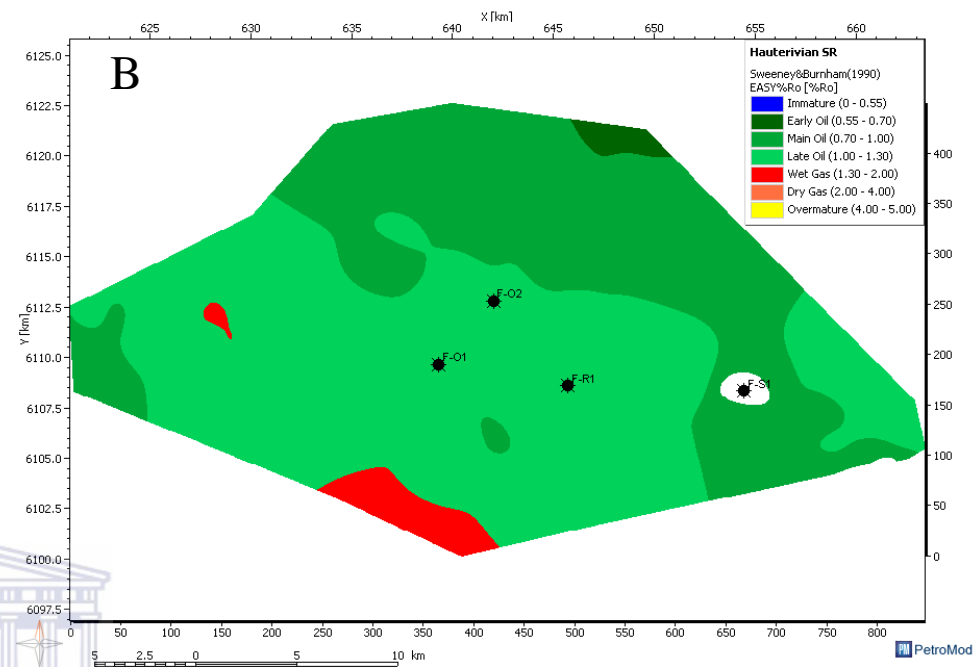
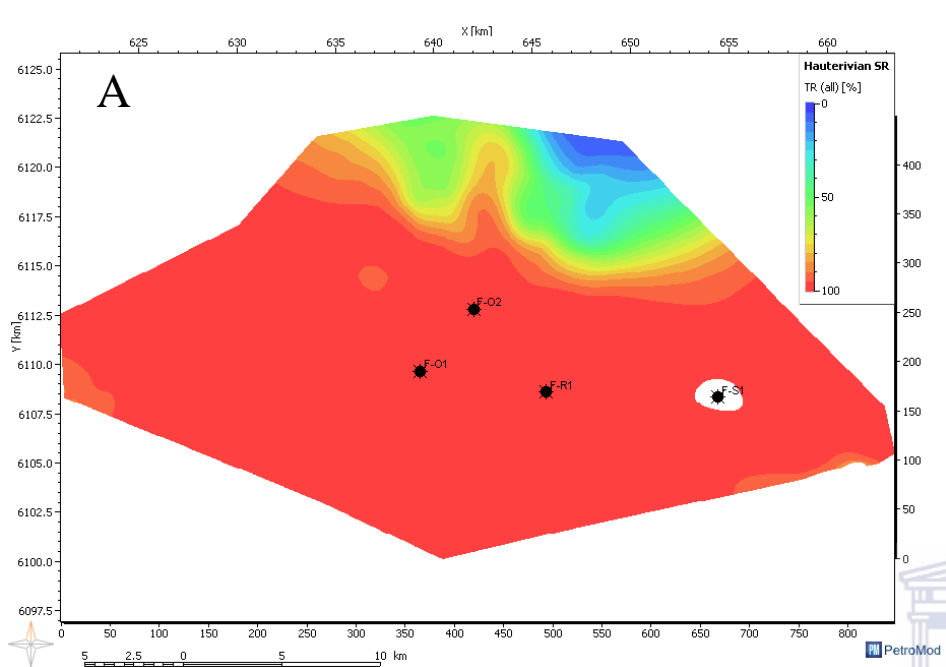
The Hauterivian source rock exhibits the highest rate of kerogen conversion, having reached mostly 100% transformation ratio with the exception of spatially limited domains in the northern domain of the modelled interval (Figure. 17A). The modelled Hauterivian intervals are mainly in the main oil (0.7-1.0% VRo) to late oil (1.0-1.3% VRo) (Figure. 17B). However, source potential for wet gas (1.3-2.0% VRo) generation is found in the western and southern portion of the source rock areal extent (Figure. 17B). The abovementioned pattern of maturity trends thus indicates a partitioning of the modelled source rocks into two maturation domains, i.e. northern and southwestern domains. As indicated by transformation ratios (TR) and vitrinite trends, the southwestern and eastern domains, is generally more mature than the northern domain (Figure. 17B).

Similar to the Hauterivian maturation trends, the mature Barremian source rock also depicts higher transformation ratios along the modelled area, with the northern domain being the exception (Figure. 17C). Higher rates of kerogen conversion reaching approximately 90-100% mostly in central and southern domains are recorded by the Barremian source rocks (Figure. 17C). The transformation ratio reached maximum in the Barremian source rock in Eocene (45 Ma) as is in the Hauterivian source rock. Present day, the Barremian source interval is mainly in the main oil (0.7-1.0% VRo) window with the northern domain still in the main oil (0.55-0.7% VRo) window (Figure. 17D). Some places in the western and southern domains are in the late oil (1.0-1.3% VRo) window. As

depicted in Figure. 17E, the modelled Aptian source rock interval has transformation ratio over 50 % with exception to the northern domain showing low transformation values. This shows that with increased burial and temperature, the Aptian source rock still can attain 100 % transformation ratio, more especially in the southwestern and eastern domains. The Aptian source interval is mainly in the main oil (0.7-1.0% VRo) window with the northern domain in the early oil (0.55-0.7% VRo) window (Figure. 17F).

The Turonian source rock has experienced the least transformation of all the source rocks (Figure. 17G). This source rock is in the early oil (0.55-0.7% VRo) window. The northern domain of the modelled area shows it has not experienced any transformation; this is also indicated in the maturity map (i.e. 0-0.55 % VRo) (Figure. 16H). It can thus be deduced that with increased burial and heat flow both the Aptian and Turonian source rocks will experience further transformation. The best match, between the measured thermal maturation data (Tmax and VRo) and the calculated maturity curve was achieved using a simple rift heat flow event with higher values during the commencement of rifting and a constant heat flow (60 mW/m^2) after the rift event. The results of this thesis show that the source rocks in this area have reached the required levels of thermal maturity to generate substantial quantities of hydrocarbons.





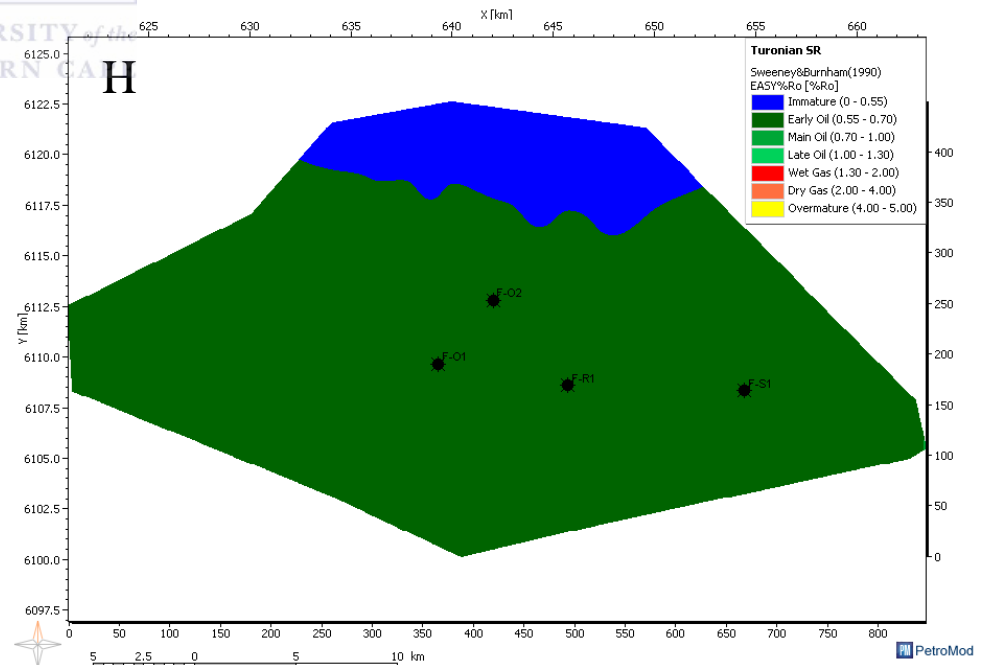
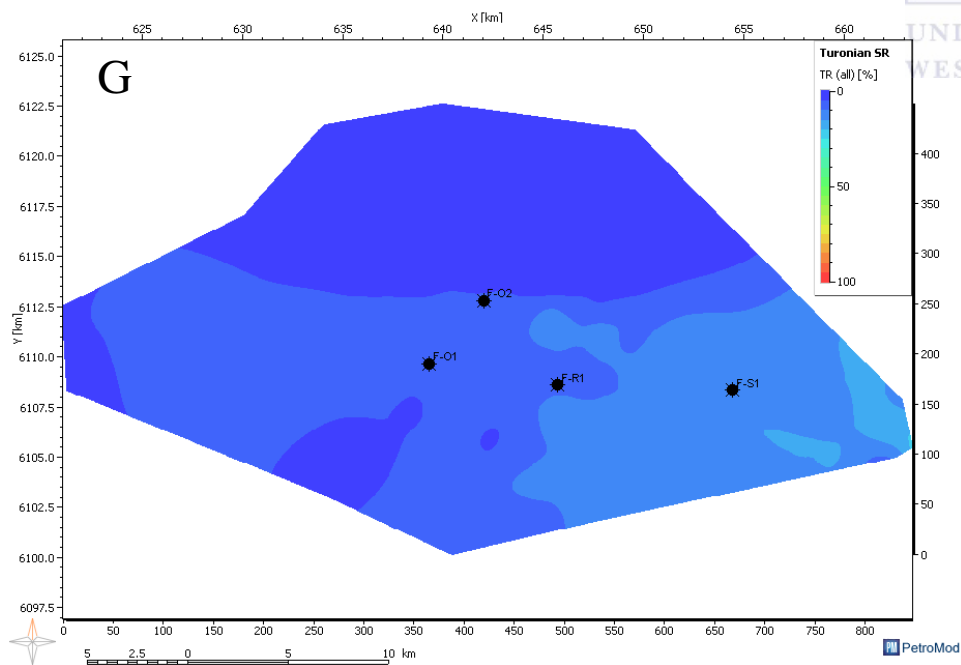
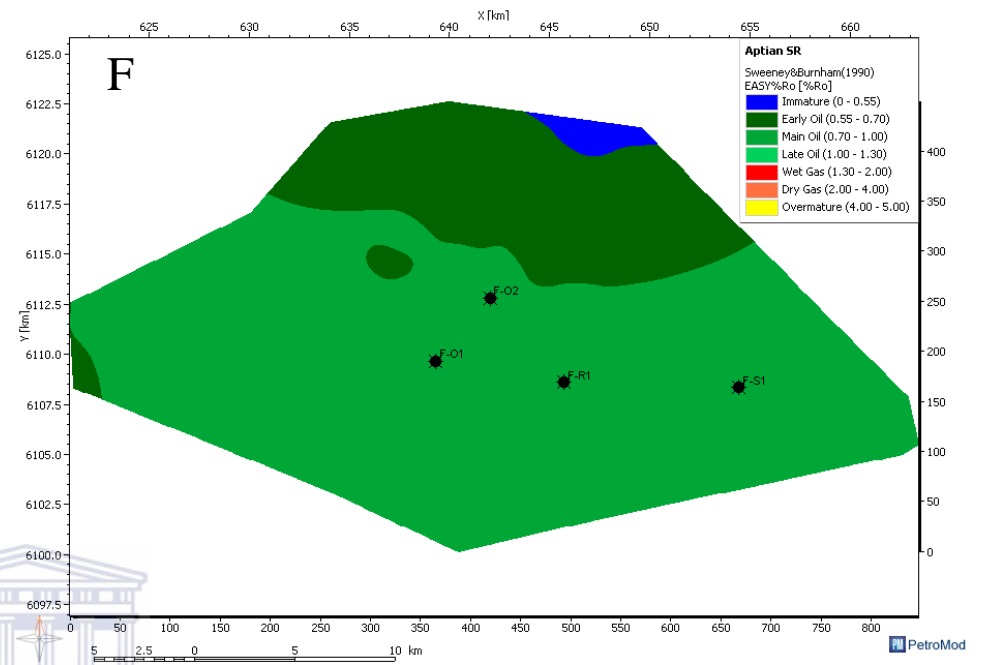
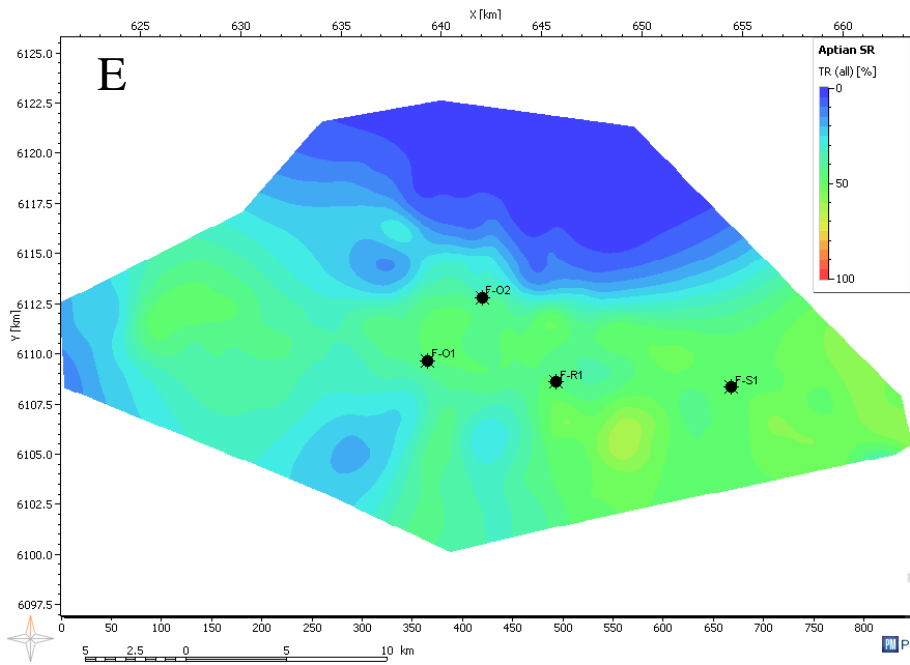


Figure 17. Transformation ratio and thermal maturity (shown as vitrinite reflectance) maps of the four source rocks presently. (A & B) Hauterivian, (C & D) Barremian, (E & F) Aptian and (G & H) Turonian.

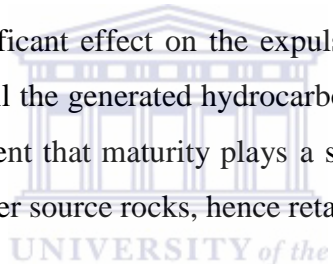
5.2 Petroleum Generation and Expulsion Efficiency

The petroleum generation shown in Figure. 18 shows the generation of hydrocarbons over time in the modelled source rocks of the F-O field. Generation begins in late Lower Cretaceous and increases over time until present age. In the model, the onset of petroleum generation takes place approximately 95 Ma, as a result of high heat flow peak and rapid subsidence/ sedimentation rates. From all the wells, it is evident that the Barremian source rock has generated the most hydrocarbons with high expulsion balance through time (Table. 5). The source rock was characterised by sharp increased hydrocarbon generation from early Upper Cretaceous (84 Ma) till Mid Eocene (45 Ma). This was then followed by a relatively constant increasing generation till present. The high generation of the Hauterivian and Barremian source rock is attributed to the high transformation ratios as shown in Figure. 17(A&C). The Aptian source rock since inception of generation shows very high generation of hydrocarbons and expulsion balance (Figure. 18), and with time and increased transformation, it has high potential to generate even more hydrocarbons. Turonian source rock shows the least hydrocarbons generation, which could be attributed to the low transformation ratio and maturity. The Hauterivian and Barremian source rocks, have low remaining potential, while the Turonian and Aptian source rocks have relatively low to high remaining potential respectively (Figure. 18)(Table. 5).

From the table below, with just 5 % transformation of the kerogen, 61 Mtons of hydrocarbons were generated by 88 Ma. In 70 Ma, 50 % transformations resulted in 605 Mtons hydrocarbons being generated. Peak generation was reached in 43 Ma with 581 Mtons of hydrocarbons generated. Presently, over 1209 Mtons hydrocarbons were generated from all the source rocks (Table. 5). The amount of accumulated hydrocarbons in each source rock is considerably low (Figure. 19). The Hauterivian, Barremian and Aptian source rocks have expulsion efficiency that is over 90% which is good because it means they are able to expel the hydrocarbons very easily. The Hauterivian source rock has expulsion efficiency of 97%. Figure. 19A shows that the hydrocarbon accumulation in Hauterivian source rock; between 84-75 Ma, the source rock reached the threshold at which it could no longer store the hydrocarbons and thus has to expel them. This corresponds to the periods of higher burial rates as seen in the burial plots (Figure. 15). Barremian source rock like the Hauterivian has high expulsion efficiency of approximately 96 %. The accumulation plot shows that generation and accumulation in the source were higher until it also reached its threshold between 84-75 Ma.

Maturity has some role in both these source rocks, because they have reached higher maturities and their expulsion efficiencies are higher, expelling almost all the hydrocarbons generated.

The accumulation plot of the Aptian source rock indicates that accumulation increased drastically from 85-75 Ma, then remained constant until 43 Ma where accumulation started to decrease. Maximum accumulation was reached around 75 Ma, but the source rock could not expel any hydrocarbons because transformation was still low. With increased transformation and generation (Figure. 18) the ability to hold hydrocarbons then decreased, thus hydrocarbons were expelled around 43 Ma causing decrease in the amount of hydrocarbons accumulated in source (Figure. 19C). Peak generation was reached around 43 Ma, which links to the time the Aptian source rock reached the threshold to hold hydrocarbons (Table. 5) as well as another period of higher burial rates (Figure. 15). The expulsion efficiency of the Aptian source rock was found to be 94 %, meaning its ability to release the hydrocarbons is very good. The higher generation of hydrocarbons by the Aptian source even though it is less mature in relation to the Hauterivian and Barremian source rocks, shows that the quantity of TOC has some significant effect on the expulsion efficiency. The Turonian source rock shows that it has accumulated all the generated hydrocarbons, hence a low expulsion efficiency of 27 %. In this case it is quite evident that maturity plays a significant role, because the Turonian has low maturity compared to the older source rocks, hence retaining all the hydrocarbons.



From all this, we can deduce that the Barremian source rock is the best source rock thus far, however the Aptian source rock though still young has produced amounts of hydrocarbons that are almost similar to Barremian source rock, thus in terms of the HI, TOC and remaining potential it is the best source rock of the four.

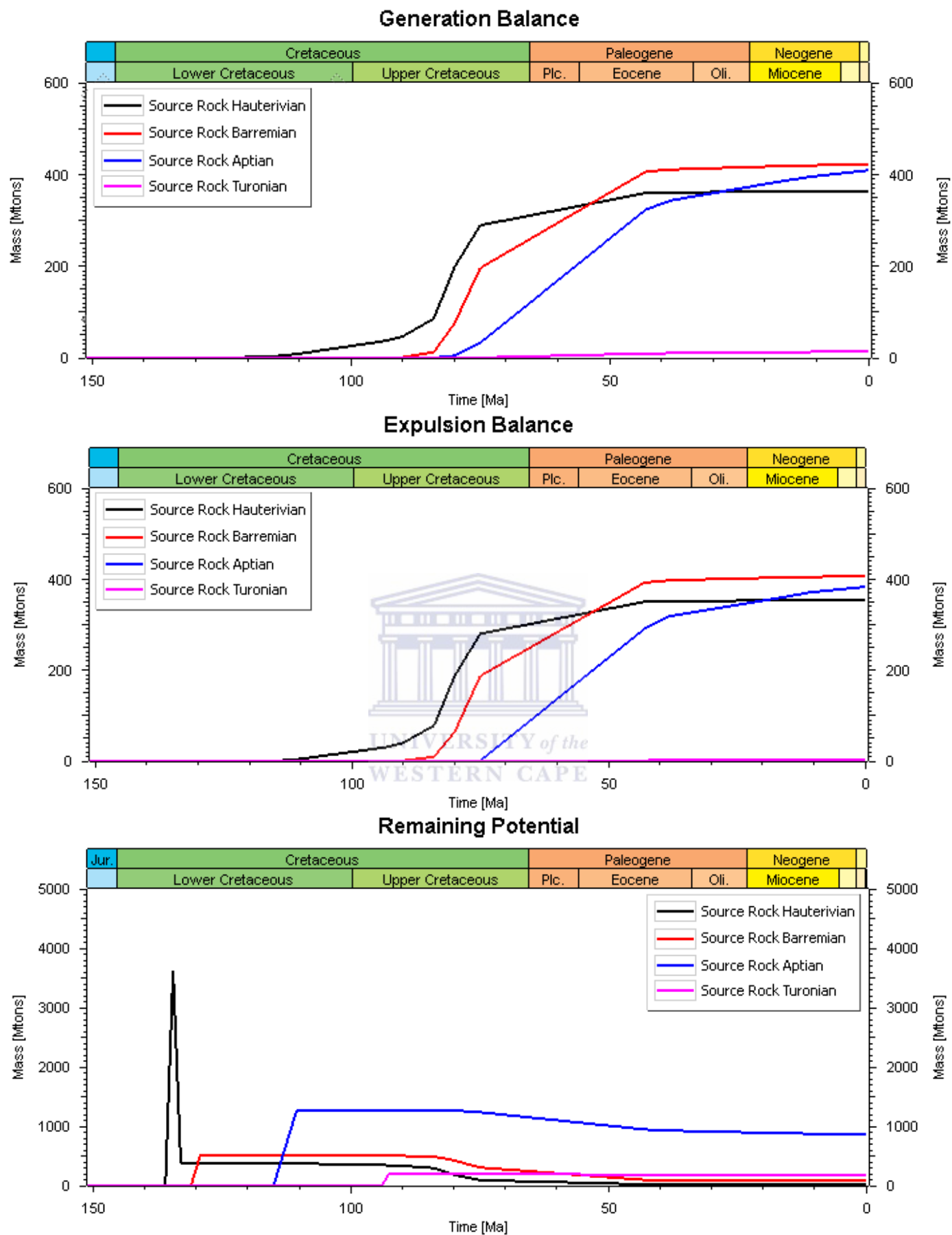


Figure 18. Results of generation, expulsion balance and remaining potential over time in all the source rocks.

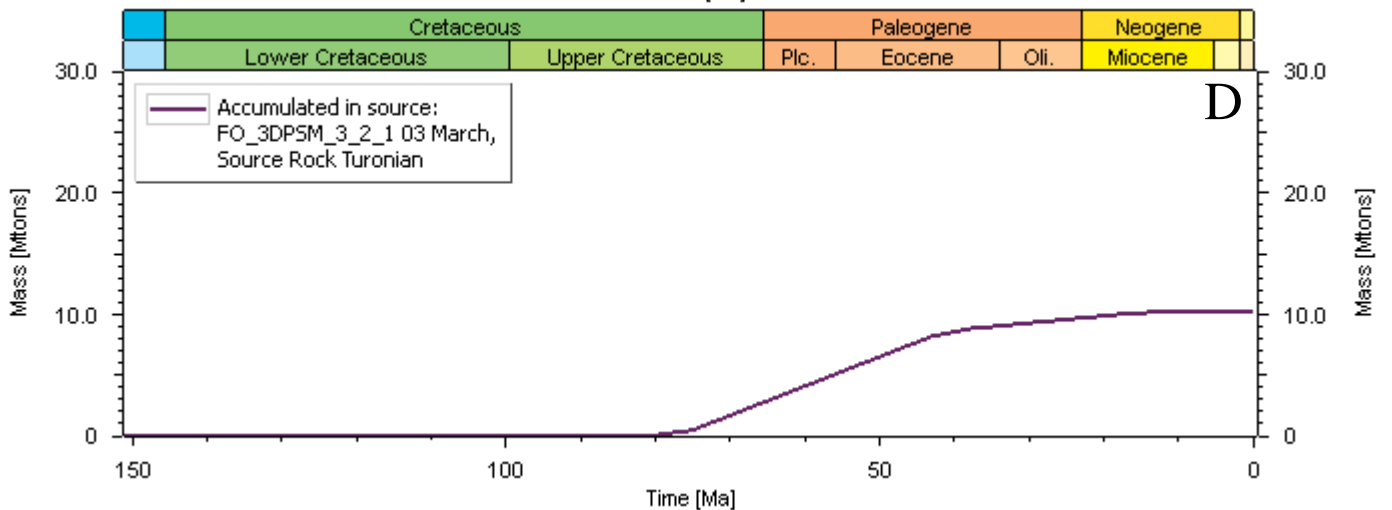
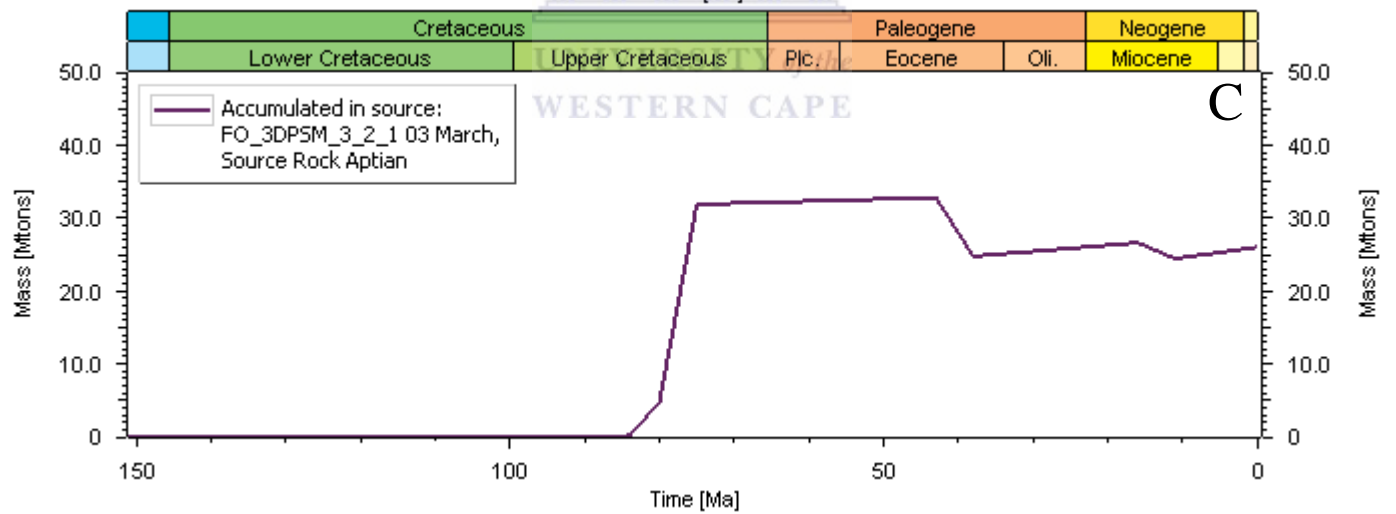
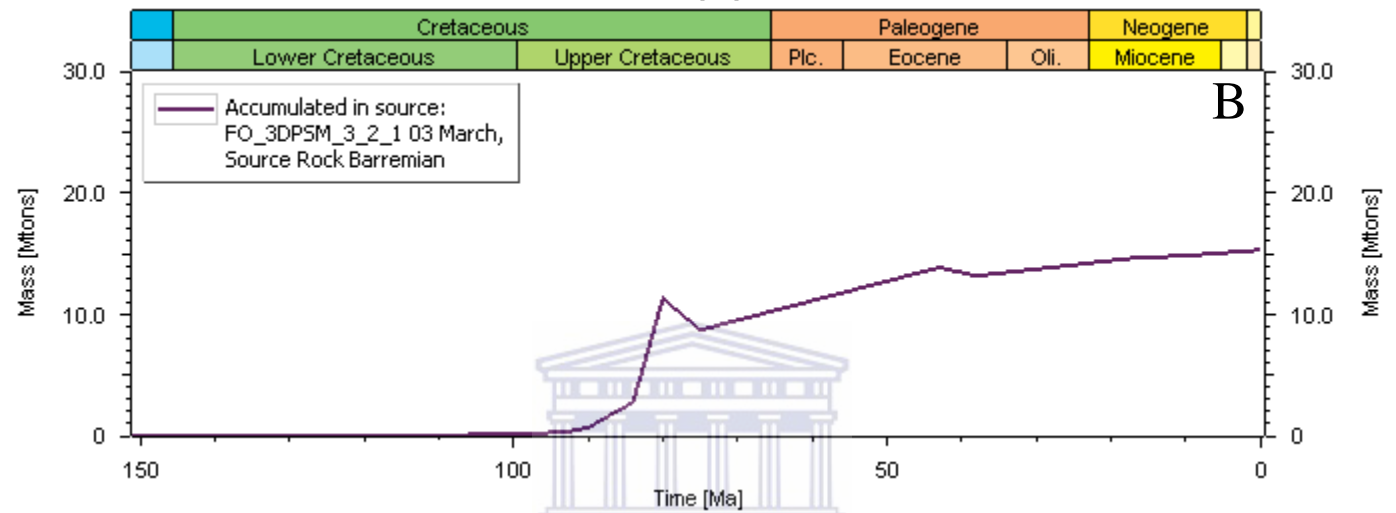
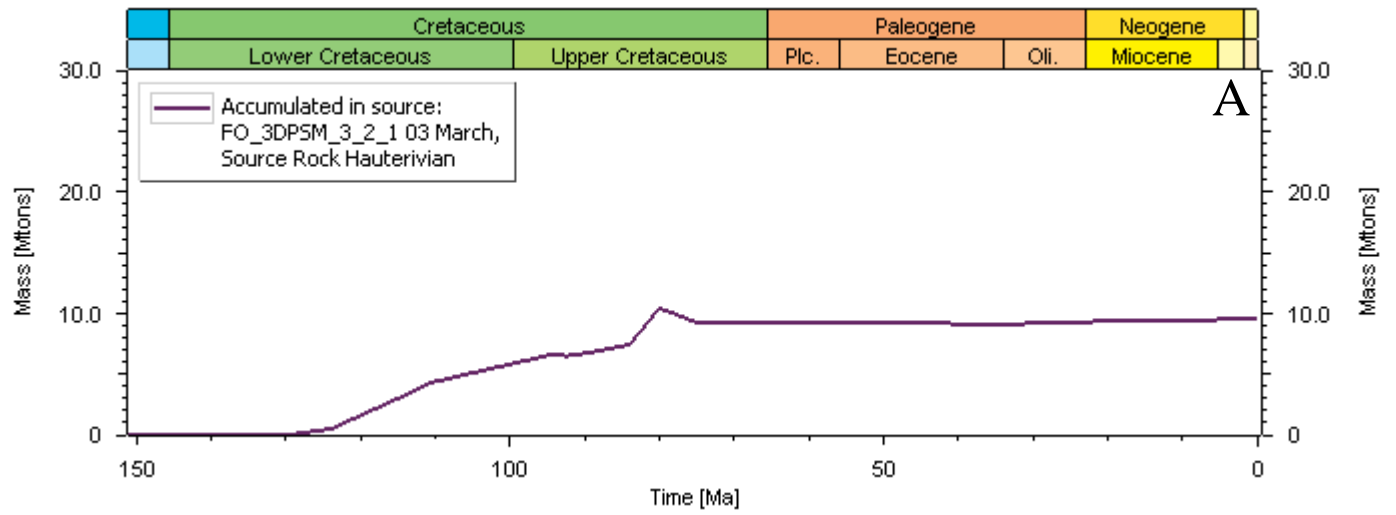


Figure 19. Cross plot showing the amount of hydrocarbons accumulated in each source rock. (A) Hauterivian, (B) Barremian, (C) Aptian and (D) Turonian.

Table 5. Table showing the amount of hydrocarbons generated and expelled over time.

Source	Generation balance	Accumulated in source	Expulsion balance	Remaining potential
Source Rock Turonian	14.15	10.22	3.93	180.83
Source Rock Aptian	409.1	25.95	383.14	861.7
Source Rock Barremian	421.72	15.29	406.44	80.97
Source Rock Hauterivian	363.53	9.52	354.01	18.24
Total	1208.5	60.97	1147.53	1141.74

Total Generation over time	Total [%]	Masses [Mtons]	Time [Ma]
	100	1209.27	0
	95	1148.81	29.03
	50	604.64	70.28
	5	60.46	88.56
	0	0	151.12
	Max Peak:	580.57	43

Chapter Six: Conclusion and Recommendations

In the present work the burial and thermal histories of F-O Gas field were modelled using temperature and vitrinite reflectance data with the use of the PetroMod software. Assumption of using simple rift heat flow consisting of higher heat flow during start of rifting and constant heat flow for post rift event for all the wells, resulted in the best fit between the measured and modelled vitrinite reflectance and bottom hole temperatures. Temperature data show that maximum temperatures reached range from 40 °C to 170 °C and the contained organic matter has reached maturities corresponding to the early oil to wet gas generation stages (as indicated by their vitrinite reflectance values). Based on modelling results, Hauterivian and Barremian source rocks have gone through higher transformation than the Aptian and Turonian source rocks. The Hauterivian source rock is situated mainly in the main and late oil window, with some oil converted to wet gas while the Barremian source rock is mainly in the main oil generation window. Aptian source rock is situated in the main oil window generation, with the northern domain in the early oil. The Turonian source rock is less mature as it is in the early oil generation window. The northern domain of the Turonian source rock is completely immature. The Barremian source rock has generated most of the hydrocarbons over time. The Aptian source rock, with the highest TOC of 3% of all the source rocks shows that with time and increased transformation it has the potential to produce even more hydrocarbons. Thus, from all the source rocks it has the highest remaining potential.

In summary, investigation of oil generation history shows that it commenced in early Cretaceous and that substantial hydrocarbons have been produced over time, with the Barremian and Aptian source rocks being the main generators of hydrocarbons with the studied F-O field. The high expulsion efficiency of the Hauterivian, Barremian and Aptian source rocks indicates that these three source rocks have expelled almost all of the hydrocarbons that were generated. The Aptian source rock has generated almost similar amount of hydrocarbons to Barremian, though it is still young and less transformed to Barremian. Due to the quality (HI) and quantity (TOC), the Aptian source rock could be regarded as the best source rock.

To further constrain source rock maturation in the study area, I would suggest testing the effects of different heat flow models. Also, migration modelling is beyond the scope of this study and therefore would be recommended to further the understanding of petroleum system evolution in the study area.

References

- Brink, G.J., Kuhlman, S., Winters, S.J., Faser, N., Basson, W. and Blagg, J., (1991). Sequence 13A, Bredasdorp Basin: A case study of the seismic/sequence stratigraphy integrated with seismic anomaly reservoir and source rock distribution trends. SOEKOR unpubl. rept. SOE-EXP-RPT-004, 33pp.
- Broad, D., (2004). South Africa activities and opportunities, an unpublished Power Point Presentation to PetroChina.
- Burnham, A. K. (1989). A simple kinetic model of petroleum formation and cracking (No. UCID-21665). Lawrence Livermore National Lab., CA (USA).
- Burden, P.L.A., (1992). Soekor, partners explore possibilities in Bredasdorp Basin off South Africa: Oil and Gas Journal, 109-115.
- Clayton, C.J., (1991a). Carbon isotope fractionation during natural gas generation from kerogen. Marine and Petroleum Geology 8 (May), 232-240.
- Daly, A.R., (1987a). Loss of organic carbon from source rocks during thermal maturation. AAPG Bulletin 71 (5), 546.
- Davies, C.P.N., (1988b). Bredasdorp Basin – south flank hydrocarbon expulsion. SOEKOR unpubl. rept., 17pp.
- Davies, C.P.N., (1997). Hydrocarbon Evolution of the Bredasdorp Basin, Offshore South Africa: From Source to Reservoir. PhD, thesis, University of Stellenbosch.
- Demaison, G.J., and Moore, G.T., (1980). Anoxic environments and oil source bed genesis. Organic Geochemistry, 2(1), 9-31.
- Dow, W.G., (1977a). Kerogen studies and geological interpretations: Journal of Geochemical exploration, v. 7, p. 79-99.
- Goutorbe, B., Lucazeau F., Bonneville, A., (2008). The thermal regime of South African continental margins. *Earth Planet. Sci. Lett.*, 267, 256–265.

Hunt, J. M., (1974). Organic geochemistry of the marine environment. *Advances in organic geochemistry*, p. 593-605

Hunt, J.M., (1991). Generation of gas and oil from coal and other terrestrial organic matter. *Organic Geochemistry*, 17 (6), 673-680.

Johnston, S.T., (2000). The Cape Fold Belt and Syntaxis and the rotated Falkland Island: dextral transpressional tectonics along the southwest margin of Gondwana. *Journal of African Earth Sciences*, 31 (1), 51-63.

Jungslager, E.H.A., (1996). The syn-rift of the Bredasdorp Basin. SOEKER unpubl. Rept. SOE-GEO-RPT- 380, 61pp.

Killops S.D., and Killops V.J., (1993). An introduction to organic geochemistry, New York, John Wiley.

Leythaeuser, D., (No Date). Origin, migration and accumulation of Petroleum. *Encyclopaedia of hydrocarbons; Volume I: Exploration, Production and Transport*. University of Koln, Germany, 66-84.

McCarthy, K., Rojas, K., Niemann, M., Palmowski, D., Peters, K., & Stankiewicz, A., (2011). Basic petroleum geochemistry for source rock evaluation. *Oilfield Review*, 23(2), 32-43.

McMillan, I.K., Brink, G.I., Broad, D.S., Maier J.J., (1997). Late Mesozoic basins off the south coast of South African. In: *African Basins* (Ed. by R. C. Selley), Elsevier, Amsterdam, 319-376.

Megner-Allogo, A.C., (2006). Sedimentology and stratigraphy of deep-water reservoirs in the 9A to 14A Sequences of the central Bredasdorp Basin, offshore South Africa (Doctoral dissertation, Stellenbosch: Stellenbosch University).

Mudaly, K., Turner, J.R., Escorcía, F., Higgs, R., (2009). F-O Gas Field, Offshore South Africa - From Integrated Approach to Field Development. AAPG international Conference and Exhibition, Cape Town, South Africa, 1-32.

Olugbemiro, R.O., (1997). Hydrocarbon Potential, maturation and Palaeoenvironments of the Cretaceous series in Bornu Basin, NE Nigeria (Doctoral dissertation, Ph. D. Thesis, Institut und Museum für Geologie und Paläontologie der Universität Tübingen, Germany, 14, 150).

Olugbemiro, O.R., and Ligouis, B., (1999). Thermal maturity and hydrocarbon potential of the Cretaceous (Cenomanian-Santonian) sediments in the Bornu (Chad) Basin, NE Nigeria. *Bulletin de la Societe Geologique de France*, 170(5), 759-772.

Petroleum Agency of South Africa (PASA), (2009). Western Bredasdorp Basin: Petroleum Agency SA Brochure, 4pp.

Petroleum Agency of South Africa (PASA), (2013). Petroleum exploration in South Africa: information and opportunities. PASA, Cape Town, 30 pp.

Schmidt, S., (2004). The petroleum potential of the passive continental margin of South-Western Africa - a basin modelling study; PhD thesis, Rheinisch-Westfälischen Technischen Hochschule Aachen, 156p.

Sonibare, W. A., Sippel, J., Scheck-Wenderoth, M., and Mikeš, D., (2015). Crust-scale 3D model of the Western Bredasdorp Basin (Southern South Africa): data-based insights from combined isostatic and 3D gravity modelling. *Basin Research*, 27(2), 125-151.

Sonibare, W.A., di Primio, R., Anka, Z., Scheck-Wenderoth, M., and Mikeš, D., (subm.). Petroleum systems evolution within a transform-related passive margin setting: crustal scale 3D basin modelling of the Western Bredasdorp Basin (Area C/West Block 9), offshore South Africa. *Marine and Petroleum Geology*.

Subseaworldnewscom, (2015). Subsea World News. Retrieved 30 September, 2015, from <http://subseaworldnews.com/2012/06/21/dcd-marine-to-supply-subsea-equipment-for-project-ikhwezi-in-south-africa/>

Sweeney, J.J., and Burnham A.K., (1990). Evaluation of a simple model of vitrinite reflectance based on chemical kinetics, *American Association of Petroleum Geology. Bulletin*, 74, 1559–1570.

Taylor, G.H., Teichmuller, M., Davis, A., Diessel, C.F.K., Littke, R., and Robert, P., (1998). *Organic Petrology. A New Handbook incorporating some revised parts of Stach's Textbook of Coal Petrology*. xvi+ 704 pp. Berlin, Stuttgart: Gebrüder Bornträger. ISBN 3 443 01036 9.

Tissot, B.P., and Welte, D.H., (1984). *Petroleum formation and occurrence*. Springer-Verlag Berlin Heidelberg, p. 679.

Van Der Spuy, D., (2003). Aptian source rocks in some South African Cretaceous basins. *Geological Society*, London, Special Publications, 207, 94-103.

Wygrala, B.P., (1989). Integrated study of an oil field in the southern Po Basin, Northern Italy, PhD thesis, University of Cologne, Germany.

